2. Feldmann, M. & Maini, R. N. (2003). Lasker Clinical Medical Research Award. TNF defined as a therapeutic target for rheumatoid arthritis and other autoimmune diseases. *Nat. Med.* **9**, 1245–1250.
3. Kooloos, W. M., de Jong, D. J., Huizinga, T. W. & Guchelaar, H. J. (2007). Potential role of pharmacogenetics in anti-TNF treatment of rheumatoid arthritis and Crohn's disease. *Drug Discov. Today*, **12**, 125–131.
4. Rutgeerts, P., Van Assche, G. & Vermeire, S. (2004). Optimizing anti-TNF treatment in inflammatory bowel disease. *Gastroenterology*, **126**, 1593–1610.
5. Rothe, J., Lesslauer, W., Lötscher, H., Lang, Y., Koebel, P., Köntgen, F. *et al.* (1993). Mice lacking the tumour necrosis factor receptor 1 are resistant to TNF-mediated toxicity but highly susceptible to infection by *Listeria monocytogenes*. *Nature*, **364**, 798–802.
6. Kafrouni, M. I., Brown, G. R. & Thiele, D. L. (2003). The role of TNF–TNFR2 interactions in generation of CTL responses and clearance of hepatic adenovirus infection. *J. Leukocyte Biol.* **74**, 564–571.
7. Rahman, M. M. & McFadden, G. (2006). Modulation of tumor necrosis factor by microbial pathogens. *PLoS Pathog.* **2**, e4.
8. Chan, F. K., Shisler, J., Bixby, J. G., Felices, M., Zheng, L., Appel, M. *et al.* (2003). A role for tumor necrosis factor receptor-2 and receptor-interacting protein in programmed necrosis and antiviral responses. *J. Biol. Chem.* **278**, 51613–51621.
9. Wajant, H., Pfizenmaier, K. & Scheurich, P. (2003). Tumor necrosis factor signaling. *Cell Death Differ.* **10**, 45–65.
10. Weiss, T., Grell, M., Siemienski, K., Mühlenbeck, F., Dürkop, H., Pfizenmaier, K. *et al.* (1998). TNFR80-dependent enhancement of TNFR60-induced cell death is mediated by TNFR-associated factor 2 and is specific for TNFR60. *J. Immunol.* **161**, 3136–3142.
11. Fotin-Mleczek, M., Henkler, F., Samel, D., Reichwein, M., Hausser, A., Parmryd, I. *et al.* (2002). Apoptotic crosstalk of TNF receptors: TNF-R2-induces depletion of TRAF2 and IAP proteins and accelerates TNF-R1-dependent activation of caspase-8. *J. Cell Sci.* **115**, 2757–2770.
12. Van Ostade, X., Vandenabeele, P., Everaerdt, B., Loetscher, H., Gentz, R., Brockhaus, M. *et al.* (1993). Human TNF mutants with selective activity on the p55 receptor. *Nature*, **361**, 266–269.
13. Barbara, J. A., Smith, W. B., Gamble, J. R., Van Ostade, X., Vandenabeele, P., Tavernier, J. *et al.* (1994). Dissociation of TNF-alpha cytotoxic and pro-inflammatory activities by p55 receptor- and p75 receptor-selective TNF-alpha mutants. *EMBO J.* **13**, 843–850.
14. Van Ostade, X., Vandenabeele, P., Tavernier, J. & Fiers, W. (1994). Human tumor necrosis factor mutants with preferential binding to and activity on either the R55 or R75 receptor. *Eur. J. Biochem.* **220**, 771–779.
15. Van Ostade, X., Tavernier, J. & Fiers, W. (1994). Structure–activity studies of human tumour necrosis factors. *Protein Eng.* **7**, 5–22.
16. Yamagishi, J., Kawashima, H., Matsuo, N., Ohue, M., Yamayoshi, M., Fukui, T. *et al.* (1990). Mutational analysis of structure–activity relationships in human tumor necrosis factor-alpha. *Protein Eng.* **3**, 713–719.
17. Zhang, X. M., Weber, I. & Chen, M. J. (1992). Site-directed mutational analysis of human tumor necrosis factor-alpha receptor binding site and structure–functional relationship. *J. Biol. Chem.* **267**, 24069–24075.
18. Banner, D. W., D'Arcy, A., Janes, W., Gentz, R., Schoenfeld, H. J., Broger, C. *et al.* (1993). Crystal structure of the soluble human 55 kD TNF receptor-human TNF beta complex: implications for TNF receptor activation. *Cell*, **73**, 431–445.
19. Fu, Z. Q., Harrison, R. W., Reed, C., Wu, J., Xue, Y. N., Chen, M. J. & Weber, I. T. (1995). Model complexes of tumor necrosis factor-alpha with receptors R1 and R2. *Protein Eng.* **8**, 1233–1241.
20. Reed, C., Fu, Z. Q., Wu, J., Xue, Y. N., Harrison, R. W., Chen, M. J. & Weber, I. T. (1997). Crystal structure of TNF-alpha mutant R31D with greater affinity for receptor R1 compared with R2. *Protein Eng.* **10**, 1101–1107.
21. Shibata, H., Yoshioka, Y., Ikemizu, S., Kobayashi, K., Yamamoto, Y., Mukai, Y. *et al.* (2004). Functionalization of tumor necrosis factor-alpha using phage display technique and PEGylation improves its anti-tumor therapeutic window. *Clin. Cancer Res.* **10**, 8293–8300.
22. Yamamoto, Y., Tsutsumi, Y., Yoshioka, Y., Nishibata, T., Kobayashi, K., Okamoto, T. *et al.* (2003). Site-specific PEGylation of a lysine-deficient TNF-alpha with full bioactivity. *Nat. Biotechnol.* **21**, 546–552.
23. Shibata, H., Yoshioka, Y., Ohkawa, A., Minowa, K., Mukai, Y., Abe, Y. *et al.* (2008). Creation and X-ray structure analysis of the tumor necrosis factor receptor-1-selective mutant of a tumor necrosis factor-alpha antagonist. *J. Biol. Chem.* **283**, 998–1007.
24. Loetscher, H., Stueber, D., Banner, D., Mackay, F. & Lesslauer, W. (1993). Human tumor necrosis factor alpha (TNF alpha) mutants with exclusive specificity for the 55-kDa or 75-kDa TNF receptors. *J. Biol. Chem.* **268**, 26350–26357.
25. Eck, M. J. & Sprang, S. R. (1989). The structure of tumor necrosis factor-alpha at 2.6 A resolution. Implications for receptor binding. *J. Biol. Chem.* **264**, 17595–17605.
26. Abe, Y., Yoshikawa, T., Kamada, H., Shibata, H., Nomura, T., Minowa, K. *et al.* (2008). Simple and highly sensitive assay system for TNFR2-mediated soluble- and transmembrane-TNF activity. *J. Immunol. Methods*, **335**, 71–78.
27. Otwinowski, Z. & Minor, W. (1997). Processing of X-ray diffraction data collected in oscillation mode. *Methods Enzymol.* **276**, 307–326.
28. Potterton, E., Briggs, P., Turkenburg, M. & Dodson, E. (2003). A graphical user interface to the CCP4 program suite. *Acta Crystallogr. Sect. D*, **59**, 1131–1137.
29. Jones, T. A., Zou, J. Y., Cowan, S. W. & Kjeldgaard, M. (1991). Improved methods for building protein models in electron density maps and the location of errors in these models. *Acta Crystallogr. Sect. A*, **47** (Pt 2), 110–119.
30. Brunger, A. T., Adams, P. D., Clore, G. M., DeLano, W. L., Gros, P., Grosse-Kunstleve, R. W. *et al.* (1998). Crystallography and NMR system: a new software suite for macromolecular structure determination. *Acta Crystallogr. Sect. D*, **54**, 905–921.

Life Sciences 83 (2008) 747–755

Contents lists available at ScienceDirect

Life Sciences

journal homepage: www.elsevier.com/locate/lifescie

Tat conjugation of adenovirus vector broadens tropism and enhances transduction efficiency

Yasuo Yoshioka [a,b,*], Ratima Asavatanabodee [b], Yusuke Eto [b], Hikaru Watanabe [b], Tomohiro Morishige [b], Xinglei Yao [b], Shinya Kida [c], Mitsuko Maeda [c], Yohei Mukai [b], Hiroyuki Mizuguchi [d,e], Koichi Kawasaki [c], Naoki Okada [b], Shinsaku Nakagawa [a,b,*]

[a] The center for Advanced Medical Engineering and Informatics, Osaka University, 1-6, Yamadaoka, Suita, Osaka, 565-0871, Japan
[b] Department of Biotechnology and Therapeutics, Graduate School of Pharmaceutical Sciences, Osaka University, 1-6, Yamadaoka, Suita, Osaka, 565-0871, Japan
[c] Faculty of Pharmaceutical Sciences, Kobe Gakuin University, Nishi-ku, Kobe 651-2180, Japan
[d] Laboratory of Gene Transfer and Regulation, National Institute of Biomedical Innovation, 7-6-8 Saito-Asagi, Ibaraki, Osaka 567-0085, Japan
[e] Graduate School of Pharmaceutical Sciences, Osaka University, 1-6, Yamadaoka, Suita, Osaka, 565-0871, Japan

ARTICLE INFO

Article history:
Received 9 May 2008
Accepted 18 September 2008

Keywords:
Adenovirus
Chemical conjugation
Gene therapy
Macropinocytosis
Protein transduction domain
The coxsackievirus
Adenovirus receptor

ABSTRACT

Aims: Adenovirus vectors (Advs) have been very useful for basic research and clinical gene therapy because they propagate to high titers and efficiently transduce cells and tissues regardless of the mitotic status. However, poor transduction of cells that lack the coxsackievirus and adenovirus receptor (CAR), the primary receptor for Advs, has limited Adv application. In this study, we attempted to generate novel Tat–Advs (Advs conjugated with the HIV Tat-derived peptide, a protein-transduction domain (PTD)) to broaden Adv tropism and enhance transduction efficiency.
Main methods: We constructed Tat–Advs by chemically conjugating Tat peptide to the surface-exposed lysine residues on Advs. We compared the gene transfer activity of Tat–Advs with that of unmodified Advs by measuring the luciferase expression in several types of cell lines.
Key findings: Tat–Advs showed gene expression 1 to 3 log orders higher than unmodified Advs in CAR-negative adherent cells and blood cells, which are refractory to conventional Advs. The inhibition of Tat–Adv-mediated gene expression by heparin and macropinocytosis inhibitor confirms that binding of Tat–Adv to cellular HSPGs and macropinocytosis are essential for efficient CAR-independent transduction. We also demonstrated that Adv modified with another PTD (R8) had the same high transduction efficiency as Tat–Adv.
Significance: These data suggest that Tat–Advs are important tools for transducing cells and will be useful as platform vectors for gene therapy.

Introduction

Gene transduction by viral vectors is currently attracting a great deal of attention for human gene therapy and the functional analysis of genes. In particular, adenovirus vectors (Advs) based on Ad type 5 have been widely used for basic research and clinical gene therapy in vivo and in vitro, because they can be propagated to high titers and efficiently transduce cells and tissues regardless of the mitotic status of the cells (Kaplan, 2005; Kawabata et al., 2006; Roth, 2006). However, the application of Adv in clinical and basic research has been limited by the native tropism of the virus. Entry of Adv into target cells depends on the presence of the coxsackievirus and adenovirus receptor (CAR; the primary receptor for Ad type 5) and integrin coreceptors on the target cells (Wickham et al., 1993; Bergelson et al., 1997; Tomko et al., 1997). Viral binding to the cell surface is mediated by binding of the adenovirus fiber to the CAR on the cells, whereas subsequent internalization occurs by binding of the Arg-Gly-Asp motif in a penton base to αv-integrins. Therefore, Adv cannot efficiently transfer genes of interest into cells lacking CAR expression (e.g., many advanced tumor cells, peripheral blood cells, and hematopoietic stem cells). It is essential to develop novel Advs with efficient transduction independent of the expression of CAR on these cells (Mizuguchi and Hayakawa, 2004; Campos and Barry, 2007).

* Corresponding authors. Yoshioka is to be contacted at The center for Advanced Medical Engineering and Informatics, Osaka University, 1-6, Yamadaoka, Suita, Osaka, 565-0871, Japan. Tel.: +81 6 6879 8177; fax: +81 6 6879 8179. Nakagawa, Department of Biotechnology and Therapeutics, Graduate School of Pharmaceutical Sciences, Osaka University, 1-6, Yamadaoka, Suita, Osaka, 565-0871, Japan. Tel.: +81 6 6879 8175; fax: +81 6 6879 8179.
E-mail addresses: yasuo@phs.osaka-u.ac.jp (Y. Yoshioka), nakagawa@phs.osaka-u.ac.jp (S. Nakagawa).

0024-3205/$ – see front matter © 2008 Elsevier Inc. All rights reserved.
doi:10.1016/j.lfs.2008.09.022

Some proteins, including Tat (transactivator of transcription) of human immunodeficiency virus and the Antennapedia homeodomain proteins of *Drosophila melanogaster* and other species, are taken up by mammalian cells via a receptor-independent unknown pathway (Frankel and Pabo, 1988; Derossi et al., 1994). The domains identified as responsible for this property are referred to as protein transduction domains (PTDs) (Kabouridis, 2003; Murriel and Dowdy, 2006). Most PTDs are 10 to 30 amino acid residues long and enriched in basic amino acids (e.g., arginine and lysine). The Tat peptide with the minimal transduction domain comprising amino acids 48 to 60 of Tat protein (GRKKRRQRRRPPQ) is the most highly investigated PTD. PTDs have been shown to mediate the efficient cellular uptake of a wide variety of cargos, including proteins, peptides, nucleic acids, and even particulates and liposomes with diameters as great as 200 nm (Schwarze et al., 1999; Lewin et al., 2000; Khalil et al., 2006). Recently, several groups reported the utility of PTDs, including the Tat peptide, in Adv-mediated gene transduction (Gratton et al., 2003; Kuhnel et al., 2004; Kurachi et al., 2007). Gratton et al. constructed a complex between Adv and Tat peptide via electrostatic interaction between the high positive charge of Tat peptide and the negative charge of the Adv capsid (Gratton et al., 2003). Their vector, however, requires a high concentration of Tat peptide for efficient gene transfer. Kuhnel et al. bound the Tat peptide to Adv by using fusion proteins consisting of CAR and Tat peptide as an adaptor to Adv (Kuhnel et al., 2004). Kurachi et al. generated genetically modified Advs that contain the Tat peptide in the HI loop of the fiber knob (Kuhnel et al., 2004; Kurachi et al., 2007). These approaches are useful for broadening the tropism of Advs and enhancing transduction efficiency independently of the CAR. However, these approaches are limited to use only with Adv and cannot be applied to other vectors. Therefore, it is important to develop a simple, general method for constructing Tat-modified vectors.

In order to broaden the tropism of Adv and enhance transduction efficiency, we previously developed a system for the synthesis of peptide with a reactive group and generated Tat peptide with 6-maleimidohexanoic acid N-hydroxysuccinimide ester (MHS) (Kida et al., 2006; Kida et al., 2007; Kida et al., 2008). We also succeeded to construct Tat-peptide-conjugated Adv (Tat–Adv) simply, by chemical conjugation of Tat peptide to the surface lysine residues of Adv (Kida et al., 2006; Kida et al., 2008). Here, to optimize Tat–Adv as a vector for gene therapy, we evaluated the relationship between Tat-peptide modification ratio and transduction efficiency. We then examined the gene transfer activities of Tat–Adv in many cell types and the mechanism of cellular uptake of Tat–Adv. We demonstrated that Tat–Adv with optimal modification ratio showed gene expression 1 to 3 log orders higher than unmodified Adv in CAR-negative adherent cells and blood cells, which are refractory to conventional Adv. Furthermore, we confirmed the involvement of the heparan sulfate proteoglycans (HSPGs) and macropinocytosis in the transduction pathway of Tat–Adv. These data suggest that Tat–Adv is an attractive tool for transducing cells and will be useful as a platform vector for gene therapy.

Materials and methods

Cells and animals

A549 cells (human lung carcinoma cells) and U937 cells (histiocytic lymphoma) were purchased from American Type Culture Collection (Manassas, VA); HEK293 (normal human embryonic kidney fibroblasts) were obtained from the Japanese Collection of Research Bioresources (Tokyo, Japan). B16BL6 cells (mouse melanoma cells) were kindly given by Kobegakuin University. CT26 cells (mouse colon carcinoma cells) were provided by Mochida Pharmaceutical Company (Tokyo, Japan). HEK293, A549, RAW264.7 and EL4 cells were cultured in Dulbecco's Modified Eagle Medium (Sigma-Aldrich, St. Louis, MO) containing 10% fetal bovine serum (FBS) and antibiotics. Human glioma cell lines, LN444 (glioblastoma multiforme), LNZ308 (glioblastoma multiforme) and SF295 (glioblastoma multiforme) cells were also cultured in Dulbecco's Modified Eagle Medium containing 10% FBS and antibiotics. B16BL6 and HeLa cells were cultured in Minimal Essential Medium (Sigma-Aldrich) containing 7.5% and 10% FBS, respectively, and antibiotics. CT26 cells were cultured in RPMI-1640 medium (Sigma-Aldrich) containing 10% FBS and antibiotics. U937 cells were cultured in RPMI-1640 medium containing 10 mM HEPES, 1 mM sodium pyruvate, 10% FBS and antibiotics. Female BALB/c mice (age, 5 weeks) were purchased from SLC Inc. (Hamamatsu, Japan). All of the animal experimental procedures were performed in accordance with the Osaka University guidelines for the welfare of animals.

Development of adenovirus vectors

E1-deleted adenovirus type 5 expressing firefly luciferase or EGFP under the control of cytomegalovirus promoter was constructed by an improved in vitro ligation method as previously reported (Mizuguchi and Kay, 1998; Mizuguchi and Kay, 1999). Each Adv was amplified in 293 cells using established methods, purified from cell lysates by banding twice through CsCl gradients, dialyzed, and stored at −80 °C (Lu et al., 1998). The virus particle titer was determined spectrophotometrically by the methods of Maizel et al. (1968). The ratio of the particle-to-biological titer was between 10 and 40.

Construction of reactive Tat peptide

The scheme used to synthesize reactive Tat peptide is shown in Fig. 1a. We used a derivative of Tat peptide containing the cross-linking reagent MHS, which reacts with amine and sulfhydryl moieties. The peptide was synthesized with an Applied Biosystems Peptide Synthesizer 433A-1 (Applied Biosystems, Foster City, CA, USA). 9-Fluorenylmethoxycarbonyl (Fmoc) amino acids [Fmoc-Gly-OH; Fmoc-Pro-OH; N^{α}-Fmoc-N^{G}-2,2,4,6,7-pentamethyldihydrobenzofuran-5-sulfonylarginine: Fmoc-Arg(Pbf)-OH; N^{α}-Fmoc-S-tritylcysteine: Fmoc-Cys(Trt)-OH; N^{α}-Fmoc-N^{ε}-t-butoxycarbonyl-lysine: Fmoc-Lys(Boc)-OH; and N^{α}-Fmoc-N^{γ}-tritylglutamine: Fmoc-Gln(Trt)-OH] were coupled in a stepwise manner to Rink amide resin (PE Biosystems. Amino content: 0.67 mequiv/g, 379 mg, 0.25 mmol) using the coupling reagent, 2-(1-H-benzotriazole-1-yl)1,1,3,3-tetramethyluronium hexafluorophosphate (HBTU), in N-methylpyrrolidone (NMP). After each coupling step, the Fmoc group was removed by using 20% piperidine/NMP. The synthetic Fmoc-Gly-Arg(Pbf)-Lys(Boc)-Lys(Boc)-Arg(Pbf)-Arg(Pbf)-Gln(Trt)-Arg(Pbf)-Arg(Pbf)-Arg(Pbf)-Pro-Pro-Gln(Trt)-Gly-Cys(Trt)-Rink amide resin was treated with 20% piperidine/NMP and then treated with acetic anhydride. The peptide was cleaved from the resin with trifluoroacetic acid (TFA)/H_2O/triisopropylsilane (95:2.5:2.5). Since synthesized peptide was deprotected and removed from resin with TFA, the ε-amino group of Lys forms the TFA salt and provided the next reaction step. The resulting crude peptide, (Ac-GRKKRRQRRRPPQGC-NH_2), was purified by RP-HPLC. The purified peptide, dissolved in PBS, and MHS, dissolved in dimethylsulfoxide, were combined and then stirred for 30 min. The product, Ac-GRKKRRQRRRPPQGC–MHS (Tat–MHS), was frozen immediately at −80 °C.

Covalent attachment of Tat to Adv

Conventional Advs were reacted with a 12.5-, 25-, 50-, or 100-fold molar excess of Tat–MHS to viral lysine residue at 37 °C for 40 min, with gentle stirring. The conjugation of Tat–MHS to Adv was determined by SDS-PAGE analysis. SDS-PAGE was carried out under reducing conditions in a gradient gel containing 4% to 20% polyacrylamide (PAG Mini 4/20, Daiichi Pure Chemicals, Tokyo, Japan) and gel was stained for the viral protein hexon by use of Coomassie blue.

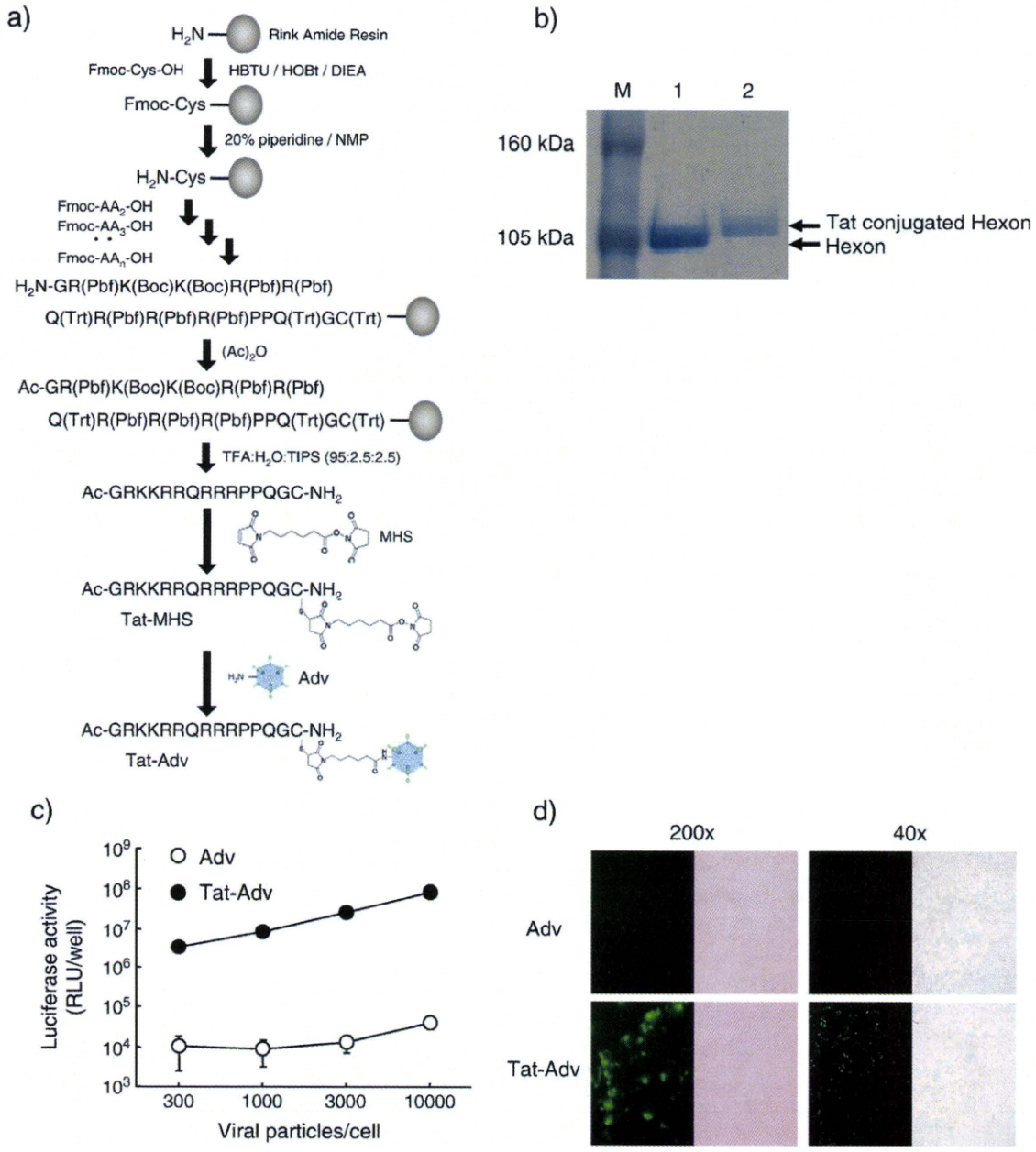

Fig. 1. Efficiency of transduction of Tat–Adv into B16BL6 cells. (a) Tat–Adv was constructed by the scheme. (b) SDS-PAGE analysis of Tat–Adv. SDS-PAGE analysis of Tat–Adv was conducted under reducing conditions and the gel was stained with Coomassie blue. Lane M, protein marker; lane 1, Adv; lanes 2, Tat–Adv. (c) B16BL6 cells (1×10^4 cells) were transduced with 300, 1000, 3000, or 10,000 vp/cell of Adv or Tat–Adv encoding the luciferase gene. After 24 h of cultivation, luciferase expression was measured. Each point represents the mean ± SD. (d) B16BL6 cells (1×10^4 cells) were transduced with 10,000 vp/cell of Adv or Tat–Adv encoding the EGFP gene. After 24 h of cultivation, EGFP expression was determined by fluorescence microscopy. Magnification, 200×, 40×.

Adenovirus-mediated gene transduction into adherent cells

Adherent cells (1×10^4 cells/well) were seeded onto a 48-well plate. On the following day, they were transduced with 300, 1000, 3000, or 10,000 vector particles (vp)/cell of Adv or Tat–Adv in a final volume of 400 μl in culture medium. After 24 h of cultivation, luciferase activity was measured with a Luciferase Assay System (Promega, Madison, WI, USA) and a Lumat LB 9507 luminometer (EG&G Berthold, Bad Wildbad, Germany) in accordance with the manufacturers' instructions after the cells had been lysed with Luciferase Cell Culture Lysis Reagent (Promega). Luciferase activity was calculated as relative light units (RLU)/well. To evaluate the expression of EGFP, B16BL6 cells (1×10^4 cells/well) were transduced with 10,000 vp/cell of Adv or Tat–Adv encoding EGFP gene. After 24 h of cultivation, expression of EGFP was measured by BZ-8000 (KEYENCE, Tokyo, Japan) Luciferase Assay System (Promega, Madison, WI, USA).

Adenovirus-mediated gene transduction into blood cells

Blood cells (2×10^4 cells/well) were seeded onto a 48-well plate. They were then transduced with 10,000 vp/cell of Adv or Tat–Adv in a final volume of 200 μl in culture medium. After 24 h cultivation, luciferase

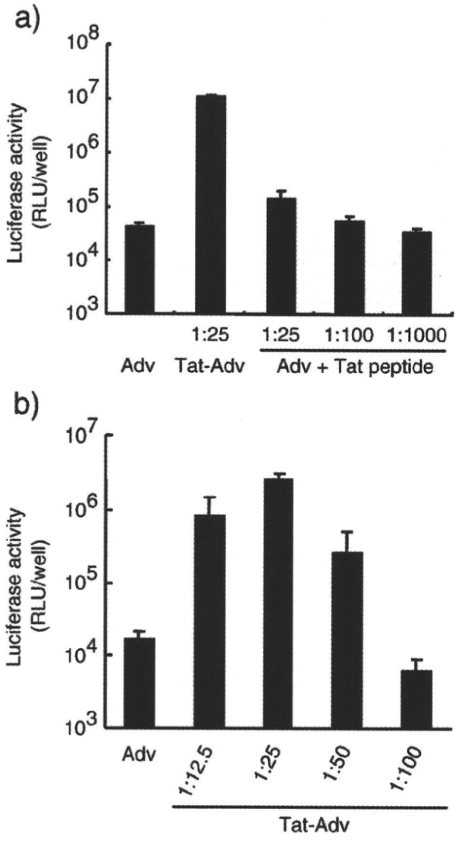

Fig. 2. Optimum condition or density of Tat peptide on the surface of Adv. (a) Comparison of efficiencies of transduction by Tat–Adv and by Adv mixed with Tat peptide containing no MHS. B16BL6 cells (1×10^4 cells) were transduced with each Adv at 10,000 vp/cell. After 24 h of cultivation, luciferase expression was measured. Each bar represents the mean±SD. Tat–Adv, molar ratio of 1:25 (Adv:Tat–MHS); Adv mixed with Tat peptide containing no MHS, molar ratios of 1:25, 1:100, 1:1000 (Adv: Tat-peptide containing no MHS). (b) Efficiency of transduction of Tat–Adv with various modification ratios. B16BL6 cells (1×10^4 cells) were transduced with Adv or Tat–Adv at 1000 vp/cell with various modification ratios. After 24 h of cultivation, luciferase expression was measured. Each bar represents the mean±SD. Tat–Adv, molar ratios of 1:12.5, 1:25, 1:50, 1:100 (Adv:Tat–MHS).

activity was measured with a Bright-Glo Luciferase Assay System (Promega) and a Lumat LB 9507 luminometer in accordance with the manufacturers' instructions. Luciferase activity was calculated as RLU/well.

Comparison of transduction efficiencies of Tat–Adv and Adv mixed with Tat peptide

B16BL6 cells (1×10^4 cells/well) were seeded onto a 48-well plate. The following day, Adv was incubated with free Tat peptides (1:25, 1:100, or 1:1000) for 40 min at 37 °C. Then, B16BL6 cells were transduced with 10,000 vp/cell of Adv, Tat–Adv, or Adv mixed with Tat-peptide containing no MHS in a final volume of 400 μl in culture medium. After 24 h cultivation, luciferase activity was measured by the Luciferase Assay System and a Lumat LB 9507 luminometer after the cells were lysed with Luciferase Cell Culture Lysis Reagent. Luciferase activity was calculated as RLU/well.

Preparation of adenovirus vector antiserum

Adv antiserum was obtained from BALB/c mice. In brief, a dose of 5×10^{10} vp of unmodified Adv was administered intravenously to a female BALB/c mouse (age, 5 weeks). Two weeks later, an additional dose of 5×10^{10} vp was intravenously administered. Mouse serum was collected after 2 weeks and stored at −80 °C.

Neutralizing antibody evasion ability of Tat–Adv

A549 cells (1×10^4 cells/well) were seeded onto a 48-well plate. The following day, the cells were transduced with 10,000 vp/cell of Adv or Tat–Adv in the presence or absence of 3200- or 12,800-fold diluted Adv antiserum (final volume, 200 μl). After 24 h of cultivation, luciferase activity was measured.

CAR dependency of cellular uptake of Tat–Adv

A549 cells (1×10^4 cells/well) were seeded onto a 48-well plate. The following day, A549 cells were pretreated with or without 1 μg/ml of mouse anti-CAR IgG (Upstate, Charlottesville, VA, USA) for 1 h. The A549 cells were then transduced with Adv or Tat–Adv at 10,000 vp/cell (final volume, 200 μl). After 24 h of cultivation, luciferase activity was measured.

HSPGs-dependency of cellular uptake of Tat–Adv

A549 cells (1×10^4 cells/well) were seeded onto a 48-well plate. The following day, the cells were transduced with Adv or Tat–Adv at 10,000 vp/cell in culture medium in the presence or absence of 6.25, 25, or 100 μg/ml of heparin sodium salt (Sigma-Aldrich) (final volume, 200 μl). After 2 h, the virus solution was replaced with fresh medium. After 24 h of cultivation, luciferase activity was measured.

Macropinocytosis-dependency of cellular uptake of Tat–Adv

A549 cells (1×10^4 cells/well) were seeded onto a 48-well plate. The following day, A549 cells were pretreated for 30 min with or without 2.5 mM amiloride HCl hydrate (Sigma-Aldrich) as a macropinocytosis inhibitor. The A549 cells were then transduced with Adv or Tat–Adv at 1000 vp/cell (final volume, 200 μl). After 30 min, the virus solution was replaced with fresh medium. After 24 h of cultivation, luciferase activity was measured.

Statistical analysis

All results are expressed as mean±SEM or SD. Differences were compared using Student *t*-tests or Scheffe's method after analysis of variance (ANOVA).

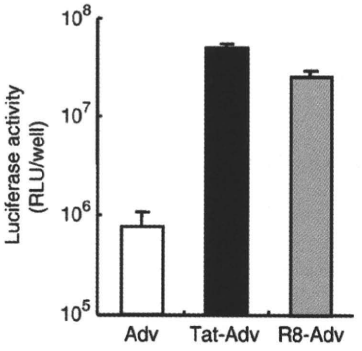

Fig. 3. Efficiency of transduction of R8–Adv. B16BL6 cells (1×10^4 cells) were transduced with 10,000 vp/cell of Adv, Tat–Adv, or R8–Adv encoding the luciferase gene. After 24 h of cultivation, luciferase expression was measured. Each bar represents the mean±SD.

Results

Generation and properties of Tat–Adv

For chemical conjugation of Tat peptide to Adv, we synthesized Tat–MHS (Fig. 1a). The Tat peptide was synthesized by the solid phase method and then coupled to the MHS. We used a derivative of Tat peptide in which cysteine residue was added to the C-terminus of the peptide. Cysteine was added so that the peptide could be linked to Adv through the heterofunctional cross-linking reagent MHS, which reacts with amine and sulfhydryl moieties. To construct Tat–Adv by using Tat–MHS, Adv was reacted with Tat–MHS at a molar ratio of 1:25 (Adv:

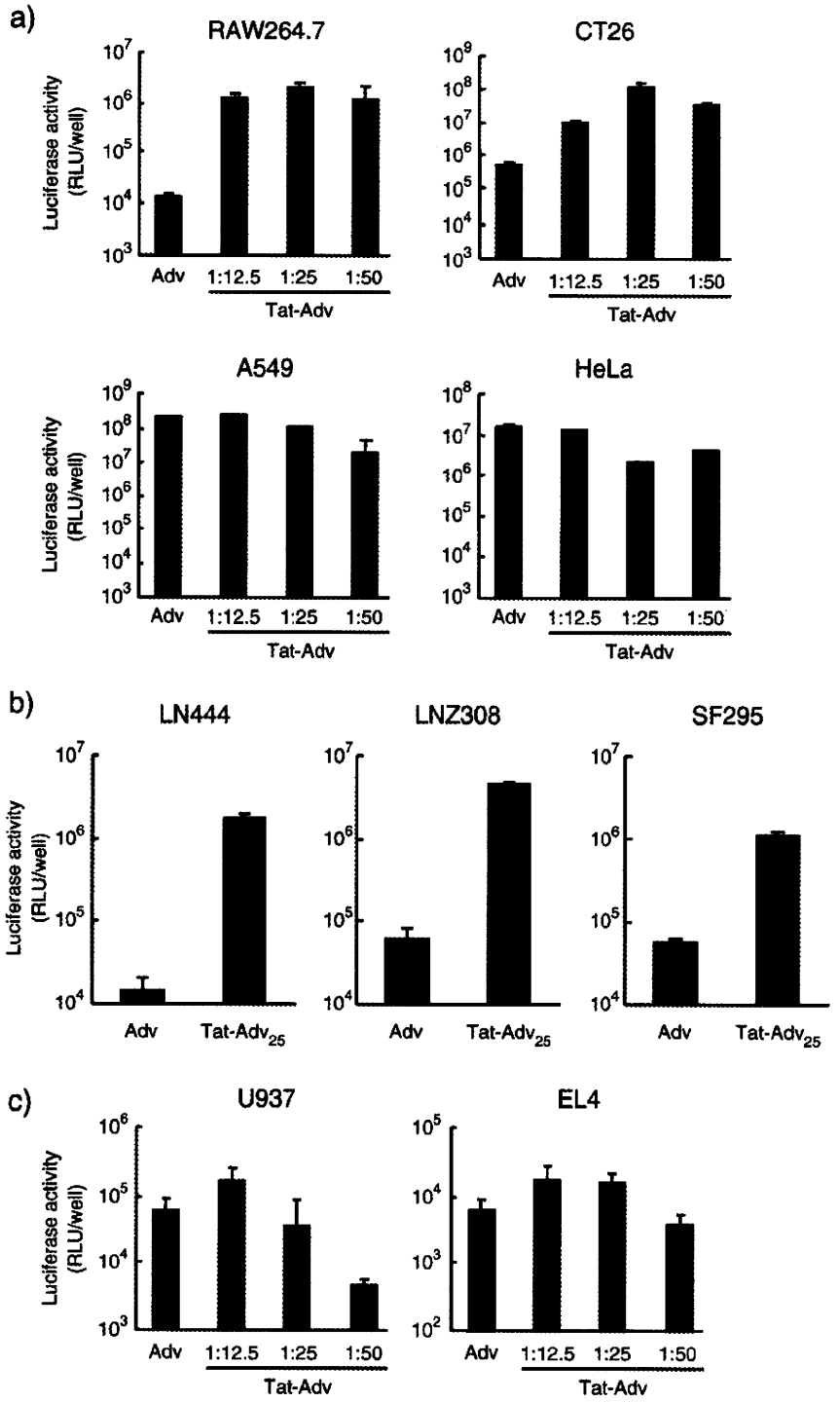

Fig. 4. Gene transfer activities of Tat–Adv in several types of cell lines. (a) RAW264.7, CT26, A549, HeLa (1×10^4 cells), (b) LN444, LNZ308, SF295 (1×10^4 cells) and (c) U937 and EL4 cells (2×10^4 cells) were transduced with 10,000 vp/cell of Adv or Tat–Adv encoding the luciferase gene. After 24 h of cultivation, luciferase expression was measured. Each bar represents the mean ± SD. Tat–Adv, molar ratio of 1:12.5, 1:25, 1:50 (Adv:Tat–MHS).

Tat–MHS) (Fig. 1a). Because conjugation of Tat–MHS to Adv results in modification of lysine residues on the capside proteins, such as the Adv hexon, fiber, and penton base, we confirmed that Tat–MHS conjugated hexon, the main capsid protein of Adv, by SDS-PAGE with Coomassie brilliant blue staining (Fig. 1b).

To investigate the transduction efficiency of Tat–Adv, we compared the gene transfer activity of Tat–Adv with that of unmodified Adv by using luciferase-expressing Advs in B16BL6 cells. B16BL6 cells are CAR-negative, and it is difficult to obtain sufficient gene expression by Adv (Koizumi et al., 2001; Koizumi et al., 2003). Tat–Adv showed 2 to 3 log orders higher luciferase expression than unmodified Adv in a vector particle-dependent manner (Fig. 1c). In addition, the efficiency of transduction in B16BL6 cells was evaluated by fluorescence microscopy using enhanced green fluorescence protein (EGFP)-expressing Advs. Visualization of cells by fluorescence microscopy showed that more Tat–Adv-treated cells than unmodified Adv-treated cells were EGFP positive (Fig. 1d). Approximately half the cells treated with Tat–Adv in the field of view showed bright-green fluorescence, whereas cells treated with unmodified Adv showed only background fluorescence. In a separate experiment, we showed that cell viability was not affected by transduction with either Adv type under these experimental conditions (data not shown).

Tat peptide is rich in basic residues and has a high positive charge. Therefore, Tat peptide should interact with the negative charge of the Adv capsid via an electrostatic interaction. To investigate the significance of direct covalent binding of Tat peptide to Adv for gene transfer, we compared the luciferase expression of Tat–Adv with that of Adv merely mixed with Tat peptide. Adv mixed with Tat peptide containing no MHS showed no increase in luciferase expression compared with unmodified Adv, whereas the luciferase expression of Tat–Adv generated by Tat–MHS at the same Tat to Adv ratio as used in the mixture was 250 times higher than that of unmodified Adv (Fig. 2a). These data indicated that direct chemical binding of Tat–MHS to Adv was essential for a high rate of transduction of Tat–Adv.

To assess the effect of Tat-peptide density on transduction efficiency, we constructed several types of Tat–Adv in which the modification ratio of the Tat peptide differed. Adv was reacted with increasing amounts of Tat–MHS; we then compared the luciferase expression in B16BL6 cells. Tat–Adv with a reaction ratio between 1:12.5 and 1:50 (Adv:Tat–MHS) showed markedly higher luciferase expression than unmodified Adv, but Tat–Adv with a reaction ratio of 1:100 (Adv:Tat–MHS) showed lower luciferase expression than unmodified Adv (Fig. 2b). These data indicated that there are optimal reaction conditions for improved transduction by Tat–Adv.

Homopolymers of arginine, called octaarginine (R8) peptide, are similar to Tat peptide in terms of efficiency and uptake mechanism, making them possible candidates for mimicking the Tat peptide (Futaki, 2005; Futaki et al., 2007). We assessed whether R8 peptide had effects similar to those of Tat peptide on Adv infection (Fig. 3). In B16BL6 cells, R8-peptide-conjugated Adv (R8–Adv) showed 30 times higher luciferase expression than unmodified Adv, indicating that higher transductional ability may be a common feature of PTDs.

Transduction efficiencies of Tat–Adv in several types of cells

Next, we examined the gene transfer activities of Tat–Adv in several types of adherent cell lines (Fig. 4a and b). We also compared the transduction efficiencies of Tat–Adv with the reaction ratios 1:12.5, 1:25, and 1:50 (Adv:Tat–MHS) (Tat–$Adv_{12.5}$, Tat–Adv_{25} and Tat–Adv_{50} respectively). Raw264.7, CT26, LN444, LNZ308 and SF295 cells were CAR-negative, whereas A549 and HeLa cells were CAR-positive (Koizumi et al., 2001; Okada et al., 2001b; Emile Gras et al., 2006). The luciferase expression in the CAR-negative adherent cell lines (Raw264.7 and CT26) transduced with Tat–Advs at any of the ratios was approximately 2 log orders higher than that observed with unmodified Adv (Fig. 4a). In the CAR-positive adherent cell lines (A549 and Hela), all Tat–Advs showed luciferase expression as efficient as that of unmodified Adv (Fig. 4a). In addition, Tat–Adv_{25} showed 1–2 log orders higher luciferase expression than unmodified Adv in CAR-negative adherent human glioma cells (LN444, LNZ308 and SF295) (Fig. 4b). Next we investigated the gene transfer activities of Tat–Advs in blood cells (U937 and EL4) (Fig. 4c). Blood cells are well known to be refractory to Adv-mediated transduction (Koizumi et al., 2001). In U937 and EL4 cells, Tat–$Adv_{12.5}$ mediated luciferase expression at a rate 3 times higher than did unmodified Adv, whereas luciferase expression by Tat–Adv_{25} and Tat–Adv_{50} was similar to, or lower than, that observed with unmodified Adv. These results indicated that Tat–Adv improved transduction efficiency in many cell types, including blood cells.

Internalization mechanisms of Tat–Adv

One potential limiting factor associated with Adv gene therapy is the existence of anti-Adv neutralizing antibodies (Abs), which limit the repeat administration of Adv (Hemminki et al., 2002; Barouch et al., 2004; Sumida et al., 2005). Most adults have low levels of anti-Adv neutralizing Abs, which hamper efficient Adv-mediated gene transfer. To investigate whether Tat–Adv was protected against anti-Adv neutralizing Abs, in vitro neutralization assay was performed to determine whether Tat–Adv had transduction efficiency in the presence of neutralizing Abs. Tat–Adv was significantly less susceptible to neutralization than unmodified Adv at both concentrations of anti-Adv serum tested (Fig. 5). This suggests that the availability of the virion surface epitopes to Abs is markedly reduced, presumably because of the shielding of antibody binding sites by Tat peptides.

To investigate the mechanism of cellular uptake of Tat–Adv, we compared the gene expression of Tat–Adv in the presence or absence of anti-CAR Ab. In CAR-positive A549 cells, luciferase expression in the cells transduced with unmodified Adv in the presence of anti-CAR Ab was 50% less than that in the absence of anti-CAR Ab. In contrast, the cells transduced with Tat–Adv in the presence of anti-CAR Ab showed a high level of gene expression similar to that in the absence of anti-CAR Ab, indicating that the cellular uptake of Tat–Adv is independent of CAR, and that Tat–Adv is taken up by the cell via an alternative mechanism (Fig. 6a). It has been shown that positively charged PTDs adhere to HSPGs on cell surfaces and that this interaction can be inhibited by negatively charged heparin (Console et al., 2003; Richard et al., 2005). Subsequent events are needed for internalization, and it has been proposed that macropinocytosis is a major pathway for the

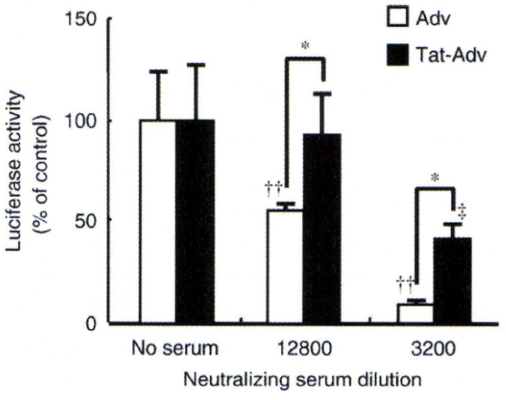

Fig. 5. Antibody evasion ability of Tat–Adv. A549 cells (1×10^4 cells) were transduced with Adv or Tat–Adv at 10,000 vp/cell in the presence or absence of Adv antiserum. After 24 h of cultivation, luciferase expression was measured. Each bar represents the mean ± SD. (*; $P<0.05$ by Student's *t*-test, ††; $P<0.01$ versus value for Adv in the absence of Adv antiserum by ANOVA, ‡; $P<0.05$ versus value for Tat–Adv in the absence of Adv antiserum by ANOVA.)

endocytic uptake of PTDs (Nakase et al., 2004; Wadia et al., 2004; Kaplan et al., 2005). To investigate the involvement of Tat binding to HSPGs in Tat–Adv-mediated transduction, we treated cells with increasing doses of heparin. Heparin significantly inhibited Tat–Adv-mediated luciferase expression in a dose-dependent manner, whereas unmodified Adv-mediated gene expression was not changed (Fig. 6b). Next, to investigate whether Tat–Adv could infect cells through macropinocytosis, we examined the effects of the macropinocytosis inhibitor amiloride on transduction efficiency. Pretreatment with amiloride decreased the luciferase expression of Tat–Adv but had no effect on the luciferase expression of unmodified Adv (Fig. 6c). The inhibition of Tat–Adv-mediated gene expression by heparin and by macropinocytosis inhibitor confirms that both binding of Tat–Adv to cellular HSPGs and macropinocytosis are essential for Tat–Adv-mediated efficient transduction.

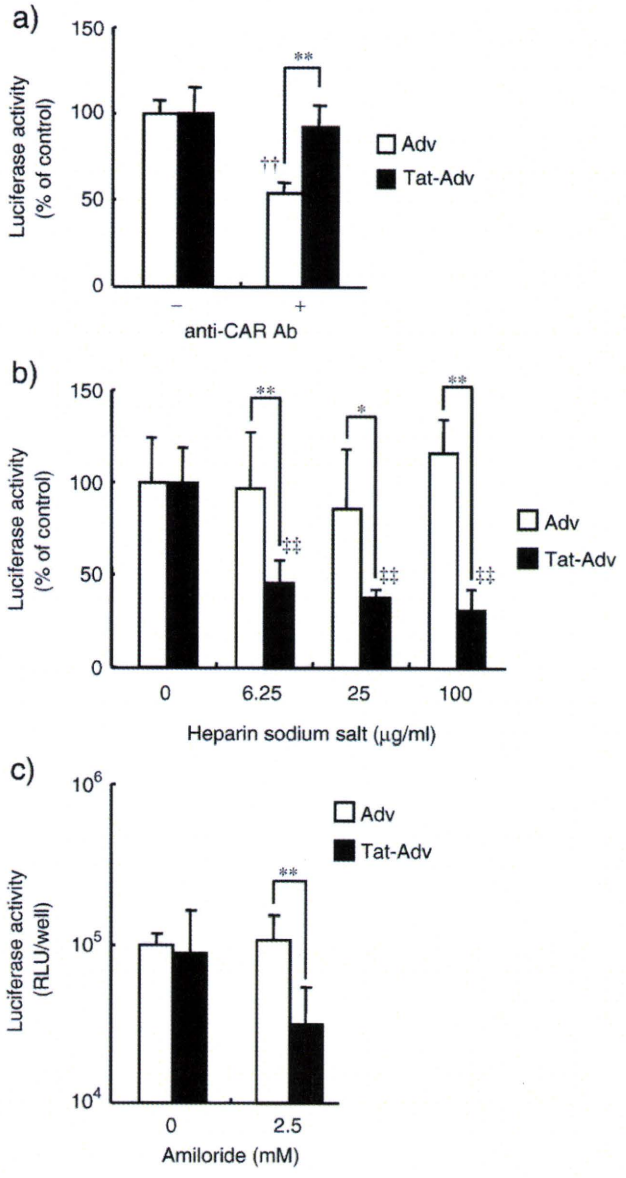

Fig. 6. Cell-entering mechanism of Tat–Adv. (a) Comparison of CAR dependency of cellular uptake of Adv and Tat–Adv. A549 cells (1×10^4 cells) were preincubated for 1 h with anti-CAR Ab at 1 μg/ml. Then, A549 cells were transduced with Adv or Tat–Adv at 10,000 particles/cell. After 24 h of cultivation, luciferase expression was measured. Each bar represents the mean±SD. (**; $P<0.01$ by Student's *t*-test, ††; $P<0.01$ versus value for Adv in the absence of anti-CAR Ab by Student's *t*-test). (b) HSPGs dependency of cellular uptake of Tat–Adv. A549 cells (1×10^4 cells) were incubated with Adv or Tat–Adv at 10,000 vp/cell in the presence or absence of heparin sodium salt at 6.25, 25, or 100 μg/ml. After 2 h, the virus solution was replaced with fresh medium. After 24 h of cultivation, luciferase expression was measured. Each bar represents the mean±SD. (*; $P<0.05$, **; $P<0.01$ by Student's *t*-test, ‡‡; $P<0.01$ versus value for Tat–Adv in the absence of heparin sodium salt by ANOVA.). (c) Macropinocytosis dependency of cellular uptake of Tat–Adv. A549 cells (1×10^4 cells) were pretreated for 30 min with or without amiloride at 2.5 mM. Then, A549 cells were transduced with Adv or Tat–Adv at 1000 vp/cell. After 30 min, the virus solution was replaced with fresh medium. After 24 h of cultivation, luciferase expression was measured. Each bar represents the mean±SD (* $P<0.05$).

Discussion

One of the hurdles confronting Adv-mediated gene transfer is that infection with Adv is dependent on the expression levels of the CAR. As a consequence, expression of the CAR determines viral tropism and frequently limits effective gene delivery by Adv. For example, because many tumor cells, including melanoma, that are targets for gene therapy express no or little CAR, it is difficult to achieve sufficient gene expression and therapeutic effect (Okada et al., 2003b; Mathis et al., 2006). Reduced expression of CAR in advanced tumor stages is one of the major obstacles to the use of Adv for cancer gene therapy (Yamamoto et al., 1997; Li et al., 1999; Yamashita et al., 2007). To overcome these problems, we developed Tat-modified Adv with broadened tropism and enhanced transduction efficiency.

Previously, we developed a system for the synthesis of peptide with a reactive group and succeeded in generating Tat–MHS (Kida et al., 2006, 2007, 2008). We prepared Tat–Adv by a simple procedure, mixing Adv with Tat–MHS (Fig. 1a). Tat–Adv showed 2 to 3 log orders higher gene expression than unmodified Adv in CAR-negative adherent cells (B16BL6, Raw264.7, CT26, LN444, LNZ308 and SF295), whereas the luciferase expression of Tat–Adv was similar to that of unmodified Adv in CAR-positive adherent cells (A549 and Hela) (Figs. 1c, 4a and b). In addition, Tat–Adv showed transgene expression several times higher than that of unmodified Adv in blood cells (U937 and EL4) (Fig. 4c). We also examined the relationship between the modification ratio of Tat peptide and transduction efficiency. Tat–Adv at reaction ratios between 1:12.5 and 1:50 (Adv:Tat–MHS) showed the highest luciferase expression, and further increases in the modification ratio of Tat peptide generated expression lower than that with unmodified Adv in B16BL6 cells (Fig. 2b). These results suggested that there is an optimum modification ratio of Tat peptide for the efficient transduction of Tat–Adv.

We focused on how the style of modification of Tat peptide affects Adv-mediated gene expression activity. We showed that modification by Tat-peptide without MHS failed to improve the transduction efficiency of Adv in B16BL6 cells (Fig. 2a). Gratton et al. obtained results opposite from ours (Gratton et al., 2003). They succeeded in improving transduction just by mixing Adv with Tat peptide containing no MHS. However, they constructed a complex between Adv and Tat peptide with a reaction ratio of 1:100,000 (Adv:peptides) – 4000 times higher than our ratio. We used Tat–Adv with a reaction ratio of 1:25 (Adv:Tat–MHS) to obtain significant effects. These results indicated that specific binding of Tat peptide to the viral particle requires less Tat peptide than when Adv is simply mixed with Tat peptide containing no MHS; this specific binding is necessary for efficient PTD-mediated transduction of Tat–Adv.

Recent data have demonstrated that internalization of Tat fusion protein and Tat-modified liposome as well as that of Tat peptide occur mainly through macropinocytosis (Nakase et al., 2004; Wadia et al., 2004; Kaplan et al., 2005; Richard et al., 2005; Khalil et al., 2006; Tunnemann et al., 2006). It has been suggested that macropinocytosis is a major pathway for the endocytic uptake of PTDs. We showed that Tat–Adv was also mainly internalized by macropinocytosis in A549 cells (Fig. 6c). Macropinocytosis involves the formation of large heterogeneous macropinosomes. Although the exact nature of Tat-mediated

release from macropinosomes into the cytosol remains unclear, macropinosomes are thought to be vesicles that are inherently leakier than other types of endosomes (Meier et al., 2002). Therefore, we speculated that the internalized Tat–Adv is easily released to the cytosol and move toward the nucleus, resulting in efficient gene expression.

Cell-surface proteoglycans such as HSPGs have been suggested to be primary receptors for the cellular uptake of PTDs, and a deficiency of HSPG often results in a decrease in the amount of PTDs taken up by the cells, although some reports have shown that HSPG is not involved in the cellular uptake of PTDs (Console et al., 2003; Richard et al., 2005; Rothbard et al., 2005; Nakase et al., 2007). Cell-surface HSPGs are also reported to be indispensable for the induction of actin organization and the macropinocytic uptake of PTDs (Nakase et al., 2004, 2007). Our results demonstrated that the presence of heparin in the medium dramatically inhibited the transduction of Tat–Adv in A549 cells (Fig. 6b), suggesting that the presence of cell-surface HSPG may be important for cellular binding and macropinocytic uptake of Tat–Adv. Recently it was shown that Tat-linked Adv, in which Tat peptide was bound to Adv by using fusion proteins consisting of CAR and the Tat peptide as an adaptor to Adv, enters the cells via HSPG (Kuhnel et al., 2004). Han et al. also showed that genetic incorporation of the Tat peptide into Adv fiber allowed to infect cells via HSPG (Han et al., 2007). These results are consistent with our observation. However, Kurachi et al. reported that the transduction of Adv genetically modified with Tat peptide, in which Tat peptide was introduced into the HI loop of the fiber knob, is not inhibited by heparinase, indicating that the genetically modified Adv transduces into the cells independently of HSPG (Kurachi et al., 2007). The precise reason for these contradictory results remains unclear. Now we are trying to examine the more precise cellular uptake mechanism of Tat–Adv using other macropinocytosis inhibitor and proteoglycan-deficient cells.

We also demonstrated that R8–Adv showed luciferase expression as high as that of Tat–Adv in B16BL6 cells (Fig. 3), indicating the usefulness of other PTDs in our PTD-conjugated Adv system. Recently, many artificial PTDs with high cell-penetrating ability have been developed (Ho et al., 2001; Mukai et al., 2006). We should be able to generate PTD-modified Advs by using these novel PTDs.

Tat–Adv has advantages over conventional Adv in many clinical applications. For example, we have shown that dendritic cell (DC)-based ex vivo immunotherapy genetically modified by Adv is useful, but the transduction efficiency of conventional Adv is insufficient for clinical use because of the lack of CAR expression on the DC surface (Okada et al., 2001a, 2003a). We consider that Tat–Adv is likely to be powerful tool for DC-based immunotherapy. In addition, for in vivo cancer gene therapy, intra-tumoral injection of Tat–Adv could enhance Adv transduction in tumor tissues and reduce side effects because of the lower dose of Adv injected, although gene transduction in vivo is affected by several cellular and humoral factors (Kurachi et al., 2007). We are now investigating the usefulness of Tat–Adv for these applications.

Conclusion

In summary, to broaden the tropism of Adv and enhance transduction efficiency, we generated Tat-modified Adv by simple chemical conjugation methods. The Tat–Adv improved transgene expression in CAR-negative cells in an HSPG- and macropinocytosis-dependent manner. This method could also be applied to other virus vectors. Tat-peptide-modified Adv is an attractive tool for transducing cells and can be useful as a platform vector for gene therapy and basic research.

Acknowledgements

The authors declare no conflict of interests. This study was supported in part by grants from the Ministry of Health, Labor, and Welfare in Japan, by the Research on Health Sciences focusing on Drug Innovation from the Japan Health Sciences Foundation and by the Mochida Memorial Foundation for Medical and Pharmaceutical Research.

References

Barouch, D.H., Pau, M.G., Custers, J.H., Koudstaal, W., Kostense, S., Havenga, M.J., Truitt, D.M., Sumida, S.M., Kishko, M.G., Arthur, J.C., Korioth-Schmitz, B., Newberg, M.H., Gorgone, D.A., Lifton, M.A., Panicali, D.L., Nabel, G.J., Letvin, N.L., Goudsmit, J., 2004. Immunogenicity of recombinant adenovirus serotype 35 vaccine in the presence of pre-existing anti-Ad5 immunity. Journal of Immunology 172, 6290–6297.

Bergelson, J.M., Cunningham, J.A., Droguett, G., Kurt-Jones, E.A., Krithivas, A., Hong, J.S., Horwitz, M.S., Crowell, R.L., Finberg, R.W., 1997. Isolation of a common receptor for Coxsackie B viruses and adenoviruses 2 and 5. Science 275, 1320–1323.

Campos, S.K., Barry, M.A., 2007. Current advances and future challenges in Adenoviral vector biology and targeting. Current Gene Therapy 7, 189–204.

Console, S., Marty, C., Garcia-Echeverria, C., Schwendener, R., Ballmer-Hofer, K., 2003. Antennapedia and HIV transactivator of transcription (TAT) "protein transduction domains" promote endocytosis of high molecular weight cargo upon binding to cell surface glycosaminoglycans. Journal of Biological Chemistry 278, 35109–35114.

Derossi, D., Joliot, A.H., Chassaing, G., Prochiantz, A., 1994. The third helix of the Antennapedia homeodomain translocates through biological membranes. Journal of Biological Chemistry 269, 10444–10450.

Emile Gras, J.C., Verkuijlen, P., Frants, R.R., Havekes, L.M., van Berkel, T.J., Biessen, E.A., van Dijk, K.W., 2006. Specific and efficient targeting of adenovirus vectors to macrophages: application of a fusion protein between an adenovirus-binding fragment and avidin, linked to a biotinylated oligonucleotide. Journal of Gene Medicine 8, 668–678.

Frankel, A.D., Pabo, C.O., 1988. Cellular uptake of the tat protein from human immunodeficiency virus. Cell 55, 1189–1193.

Futaki, S., 2005. Membrane-permeable arginine-rich peptides and the translocation mechanisms. Advanced Drug Delivery Reviews 57, 547–558.

Futaki, S., Nakase, I., Tadokoro, A., Takeuchi, T., Jones, A.T., 2007. Arginine-rich peptides and their internalization mechanisms. Biochemical Society Transactions 35, 784–787.

Gratton, J.P., Yu, J., Griffith, J.W., Babbitt, R.W., Scotland, R.S., Hickey, R., Giordano, F.J., Sessa, W.C., 2003. Cell-permeable peptides improve cellular uptake and therapeutic gene delivery of replication-deficient viruses in cells and in vivo. Natural Medicines 9, 357–362.

Han, T., Tang, Y., Ugai, H., Perry, L.E., Siegal, G.P., Contreras, J.L., Wu, H., 2007. Genetic incorporation of the protein transduction domain of Tat into Ad5 fiber enhances gene transfer efficacy. Journal of Virology 4, 103.

Hemminki, A., Wang, M., Desmond, R.A., Strong, T.V., Alvarez, R.D., Curiel, D.T., 2002. Serum and ascites neutralizing antibodies in ovarian cancer patients treated with intraperitoneal adenoviral gene therapy. Human Gene Therapy 13, 1505–1514.

Ho, A., Schwarze, S.R., Mermelstein, S.J., Waksman, G., Dowdy, S.F., 2001. Synthetic protein transduction domains: enhanced transduction potential in vitro and in vivo. Cancer Research 61, 474–477.

Kabouridis, P.S., 2003. Biological applications of protein transduction technology. Trends in Biotechnology 21, 498–503.

Kaplan, J.M., 2005. Adenovirus-based cancer gene therapy. Current Gene Therapy 5, 595–605.

Kaplan, I.M., Wadia, J.S., Dowdy, S.F., 2005. Cationic TAT peptide transduction domain enters cells by macropinocytosis. Journal of Controlled Release 102, 247–253.

Kawabata, K., Sakurai, F., Koizumi, N., Hayakawa, T., Mizuguchi, H., 2006. Adenovirus vector-mediated gene transfer into stem cells. Molecular Pharmacology 3, 95–103.

Khalil, I.A., Kogure, K., Futaki, S., Harashima, H., 2006. High density of octaarginine stimulates macropinocytosis leading to efficient intracellular trafficking for gene expression. Journal of Biological Chemistry 281, 3544–3551.

Kida, S., Maeda, M., Hojo, K., Eto, Y., Gao, J.Q., Kurachi, S., Mizuguchi, H., Hayakawa, T., Mayumi, T., Nakagawa, S., Kawasaki, K., 2006. Design and synthesis of a Tat-related gene transporter: a tool for carrying the adenovirus vector into cells. Bioorganic & Medicinal Chemistry Letters 16, 743–745.

Kida, S., Maeda, M., Hojo, K., Eto, Y., Nakagawa, S., Kawasaki, K., 2007. Studies on heterobifunctional cross-linking reagents, 6-maleimidohexanoic acid active esters. Chemical and Pharmaceutical Bulletin (Tokyo) 55, 685–687.

Kida, S., Eto, Y., Maeda, M., Yoshioka, Y., Nakagawa, S., Hojo, K., Tsuda, Y., Mayumia, T., Kawasaki, K., 2008. Preparation of a tat-related transporter peptide for carrying the adenovirus vector into cells. Protein Peptide Letters 15, 219–222.

Koizumi, N., Mizuguchi, H., Hosono, T., Ishii-Watabe, A., Uchida, E., Utoguchi, N., Watanabe, Y., Hayakawa, T., 2001. Efficient gene transfer by fiber-mutant adenoviral vectors containing RGD peptide. Biochimica et Biophysica Acta 1568, 13–20.

Koizumi, N., Mizuguchi, H., Utoguchi, N., Watanabe, Y., Hayakawa, T., 2003. Generation of fiber-modified adenovirus vectors containing heterologous peptides in both the HI loop and C terminus of the fiber knob. Journal of Gene Medicine 5, 267–276.

Kuhnel, F., Schulte, B., Wirth, T., Woller, N., Schafers, S., Zender, L., Manns, M., Kubicka, S., 2004. Protein transduction domains fused to virus receptors improve cellular virus uptake and enhance oncolysis by tumor-specific replicating vectors. Journal of Virology 78, 13743–13754.

Kurachi, S., Tashiro, K., Sakurai, F., Sakurai, H., Kawabata, K., Yayama, K., Okamoto, H., Nakagawa, S., Mizuguchi, H., 2007. Fiber-modified adenovirus vectors containing the TAT peptide derived from HIV-1 in the fiber knob have efficient gene transfer activity. Gene Therapy 14, 1160–1165.

Lewin, M., Carlesso, N., Tung, C.H., Tang, X.W., Cory, D., Scadden, D.T., Weissleder, R., 2000. Tat peptide-derivatized magnetic nanoparticles allow in vivo tracking and recovery of progenitor cells. Nature Biotechnology 18, 410–414.

Li, Y., Pong, R.C., Bergelson, J.M., Hall, M.C., Sagalowsky, A.I., Tseng, C.P., Wang, Z., Hsieh, J.T., 1999. Loss of adenoviral receptor expression in human bladder cancer cells: a potential impact on the efficacy of gene therapy. Cancer Research 59, 325–330.

Lu, Y., Zhang, Y., Steiner, M.S., 1998. Efficient identification of recombinant adenoviruses by direct plaque screening. DNA and Cell Biology 17, 643–645.
Maizel Jr., J.V., White, D.O., Scharff, M.D., 1968. The polypeptides of adenovirus. I. Evidence for multiple protein components in the virion and a comparison of types 2, 7A, and 12. Virology 36, 115–125.
Mathis, J.M., Stewart, P.L., Zhu, Z.B., Curiel, D.T., 2006. Advanced generation adenoviral virotherapy agents embody enhanced potency based upon CAR-independent tropism. Clinical Cancer Research 12, 2651–2656.
Meier, O., Boucke, K., Hammer, S.V., Keller, S., Stidwill, R.P., Hemmi, S., Greber, U.F., 2002. Adenovirus triggers macropinocytosis and endosomal leakage together with its clathrin-mediated uptake. Journal of Cell Biology 158, 1119–1131.
Mizuguchi, H., Hayakawa, T., 2004. Targeted adenovirus vectors. Human Gene Therapy 15, 1034–1044.
Mizuguchi, H., Kay, M.A., 1998. Efficient construction of a recombinant adenovirus vector by an improved in vitro ligation method. Human Gene Therapy 9, 2577–2583.
Mizuguchi, H., Kay, M.A., 1999. A simple method for constructing E1- and E1/E4-deleted recombinant adenoviral vectors. Human Gene Therapy 10, 2013–2017.
Mukai, Y., Sugita, T., Yamato, T., Yamanada, N., Shibata, H., Imai, S., Abe, Y., Nagano, K., Nomura, T., Tsutsumi, Y., Kamada, H., Nakagawa, S., Tsunoda, S., 2006. Creation of novel Protein Transduction Domain (PTD) mutants by a phage display-based high-throughput screening system. Biological & Pharmaceutical Bulletin 29, 1570–1574.
Murriel, C.L., Dowdy, S.F., 2006. Influence of protein transduction domains on intracellular delivery of macromolecules. Expert Opinion in Drug Delivery 3, 739–746.
Nakase, I., Niwa, M., Takeuchi, T., Sonomura, K., Kawabata, N., Koike, Y., Takehashi, M., Tanaka, S., Ueda, K., Simpson, J.C., Jones, A.T., Sugiura, Y., Futaki, S., 2004. Cellular uptake of arginine-rich peptides: roles for macropinocytosis and actin rearrangement. Molecular Therapy 10, 1011–1022.
Nakase, I., Tadokoro, A., Kawabata, N., Takeuchi, T., Katoh, H., Hiramoto, K., Negishi, M., Nomizu, M., Sugiura, Y., Futaki, S., 2007. Interaction of arginine-rich peptides with membrane-associated proteoglycans is crucial for induction of actin organization and macropinocytosis. Biochemistry 46, 492–501.
Okada, N., Saito, T., Masunaga, Y., Tsukada, Y., Nakagawa, S., Mizuguchi, H., Mori, K., Okada, Y., Fujita, T., Hayakawa, T., Mayumi, T., Yamamoto, A., 2001a. Efficient antigen gene transduction using Arg-Gly-Asp fiber-mutant adenovirus vectors can potentiate antitumor vaccine efficacy and maturation of murine dendritic cells. Cancer Research 61, 7913–7919.
Okada, N., Tsukada, Y., Nakagawa, S., Mizuguchi, H., Mori, K., Saito, T., Fujita, T., Yamamoto, A., Hayakawa, T., Mayumi, T., 2001b. Efficient gene delivery into dendritic cells by fiber-mutant adenovirus vectors. Biochemical and Biophysical Research Communications 282, 173–179.
Okada, N., Masunaga, Y., Okada, Y., Mizuguchi, H., Iiyama, S., Mori, N., Sasaki, A., Nakagawa, S., Mayumi, T., Hayakawa, T., Fujita, T., Yamamoto, A., 2003a. Dendritic cells transduced with gp100 gene by RGD fiber-mutant adenovirus vectors are highly efficacious in generating anti-B16BL6 melanoma immunity in mice. Gene Therapy 10, 1891–1902.
Okada, Y., Okada, N., Mizuguchi, H., Hayakawa, T., Mayumi, T., Mizuno, N., 2003b. An investigation of adverse effects caused by the injection of high-dose TNFalpha-expressing adenovirus vector into established murine melanoma. Gene Therapy 10, 700–705.
Richard, J.P., Melikov, K., Brooks, H., Prevot, P., Lebleu, B., Chernomordik, L.V., 2005. Cellular uptake of unconjugated TAT peptide involves clathrin-dependent endocytosis and heparan sulfate receptors. Journal of Biological Chemistry 280, 15300–15306.
Roth, J.A., 2006. Adenovirus p53 gene therapy. Expert Opinion on Biological Therapy 6, 55–61.
Rothbard, J.B., Jessop, T.C., Wender, P.A., 2005. Adaptive translocation: the role of hydrogen bonding and membrane potential in the uptake of guanidinium-rich transporters into cells. Advanced Drug Delivery Reviews 57, 495–504.
Schwarze, S.R., Ho, A., Vocero-Akbani, A., Dowdy, S.F., 1999. In vivo protein transduction: delivery of a biologically active protein into the mouse. Science 285, 1569–1572.
Sumida, S.M., Truitt, D.M., Lemckert, A.A., Vogels, R., Custers, J.H., Addo, M.M., Lockman, S., Peter, T., Peyerl, F.W., Kishko, M.G., Jackson, S.S., Gorgone, D.A., Lifton, M.A., Essex, M., Walker, B.D., Goudsmit, J., Havenga, M.J., Barouch, D.H., 2005. Neutralizing antibodies to adenovirus serotype 5 vaccine vectors are directed primarily against the adenovirus hexon protein. Journal of Immunology 174, 7179–7185.
Tomko, R.P., Xu, R., Philipson, L., 1997. HCAR and MCAR: the human and mouse cellular receptors for subgroup C adenoviruses and group B coxsackieviruses. Proceedings of the National Academy of Sciences of the United States of America 94, 3352–3356.
Tunnemann, G., Martin, R.M., Haupt, S., Patsch, C., Edenhofer, F., Cardoso, M.C., 2006. Cargo-dependent mode of uptake and bioavailability of TAT-containing proteins and peptides in living cells. FASEB Journal 20, 1775–1784.
Wadia, J.S., Stan, R.V., Dowdy, S.F., 2004. Transducible TAT-HA fusogenic peptide enhances escape of TAT-fusion proteins after lipid raft macropinocytosis. Natural Medicines 10, 310–315.
Wickham, T.J., Mathias, P., Cheresh, D.A., Nemerow, G.R., 1993. Integrins alpha v beta 3 and alpha v beta 5 promote adenovirus internalization but not virus attachment. Cell 73, 309–319.
Yamamoto, H., Itoh, F., Sakamoto, H., Nakajima, Y., Une, Y., Hinoda, Y., Imai, K., 1997. Association of reduced cell adhesion regulator messenger RNA expression with tumor progression in human hepatocellular carcinoma. International Journal of Cancer 74, 251–254.
Yamashita, M., Ino, A., Kawabata, K., Sakurai, F., Mizuguchi, H., 2007. Expression of coxsackie and adenovirus receptor reduces the lung metastatic potential of murine tumor cells. International Journal of Cancer 121, 1690–1696.

Biochemical and Biophysical Research Communications 384 (2009) 296–300

Contents lists available at ScienceDirect

Biochemical and Biophysical Research Communications

journal homepage: www.elsevier.com/locate/ybbrc

TNF superfamily member, TL1A, is a potential mucosal vaccine adjuvant

Hiroyuki Kayamuro [a,b,1], Yasuo Yoshioka [a,c,1], Yasuhiro Abe [a,1], Kazufumi Katayama [d], Tokuyuki Yoshida [a,b], Kohei Yamashita [a,b], Tomoaki Yoshikawa [a,b], Takachika Hiroi [d], Norio Itoh [c], Yuichi Kawai [e], Tadanori Mayumi [e], Haruhiko Kamada [a,c], Shin-ichi Tsunoda [a,c,*], Yasuo Tsutsumi [a,b,c]

[a] Laboratory of Pharmaceutical Proteomics, National Institute of Biomedical Innovation (NiBio), 7-6-8 Saito-Asagi, Ibaraki, Osaka 567-0085, Japan
[b] Graduate School of Pharmaceutical Sciences, Osaka University, 1-6 Yamadaoka, Suita, Osaka 565-0871, Japan
[c] The Center for Advanced Medical Engineering and Informatics, Osaka University, 1-6 Yamadaoka, Suita, Osaka 565-0871, Japan
[d] Department of Allergy and Immunology, The Tokyo Metropolitan Institute of Medical Science, 3-18-22 Honkomagome, Bunkyo-ku, Tokyo 113-8613, Japan
[e] Faculty of Pharmaceutical Sciences, Kobe-Gakuin University, 518, Arise, Ikawadani, Nishiku, Kobe 651-2180, Japan

ARTICLE INFO

Article history:
Received 17 April 2009
Available online 4 May 2009

Keywords:
Cytokine
IgA
Mucosal immunity
Vaccine

ABSTRACT

The identification of cytokine adjuvants capable of inducing an efficient mucosal immune response against viral pathogens has been long anticipated. Here, we attempted to identify the potential of tumor necrosis factor superfamily (TNFS) cytokines to function as mucosal vaccine adjuvants. Sixteen different TNFS cytokines were used to screen mucosal vaccine adjuvants, after which their immune responses were compared. Among the TNFS cytokines, intranasal immunization with OVA plus APRIL, TL1A, and TNF-α exhibited stronger immune response than those immunized with OVA alone. TL1A induced the strongest immune response and augmented OVA-specific IgG and IgA responses in serum and mucosal compartments, respectively. The OVA-specific immune response of TL1A was characterized by high levels of serum IgG1 and increased production of IL-4 and IL-5 from splenocytes of immunized mice, suggesting that TL1A might induce Th2-type responses. These findings indicate that TL1A has the most potential as a mucosal adjuvant among the TNFS cytokines.

Introduction

The majority of infectious pathogens, including HIV or influenza virus, enter through a mucosal surface. One important aspect of the immune response at mucosal surfaces is the production of secretory immunoglobulin (Ig) A antibodies, as well as the induction of cytotoxic T cells (CTLs) against epithelium-transmitted pathogens; therefore, the development of vaccines that induce effective immune responses at mucosal surfaces is important.

Mucosal vaccines administered either orally or nasally are highly warranted in order to combat these infectious diseases, as they would reduce the transmission of infectious pathogens more efficiently than parenteral administration by stimulating both mucosal and systemic immune responses [1,2]. The mucosal antigen-specific immune response, however, is weak because most protein antigens, such as non-living macromolecules or protein-subunit antigens, evoke only a weak or undetectable adaptive immune response when they are applied mucosally. Therefore, in order to develop mucosal vaccines, it is necessary to develop a mucosal vaccine adjuvant [3]. Both the cholera toxin and *Escherichia coli* heat-labile toxin are potent mucosal vaccine adjuvants, which have been used in experimental systems. Unfortunately, the watery diarrhea induced by these toxins makes their use as oral adjuvants clinically problematic to humans [4]. In addition, recent reports showed that a human vaccine containing inactivated influenza virus and the heat-labile toxin as an adjuvant resulted in a very high incidence of Bell's palsy [5]. Therefore, mucosal vaccine adjuvants with high efficacy and safety for the purpose of a clinical application are necessary.

Cytokines can trigger the innate and adaptive immune responses and also synergize with costimulatory molecules to improve the immune response. Therefore, cytokines are promising vaccine adjuvants that enhance the immune response against pathogens. The members of the tumor necrosis factor (TNF)/TNF receptor (TNFR) superfamily are critically involved in maintaining the homeostasis of the immune system [6–8]. Currently, more than 40 members of the TNF/TNFR superfamily have been identified and the majority is expressed by immune cells. The biological functions of this system encompass beneficial and protective effects in inflammation and host defense as well as a crucial role in immune organogenesis [7]. Among TNF superfamily cytokines, there are some candidates used as vaccine adjuvants to enhance the primary and memory immune responses against cancer and infectious

* Corresponding author. Address: National Institute of Biomedical Innovation (NiBio), 7-6-8 Saito-Asagi, Ibaraki, Osaka 567-0085, Japan. Fax: +81 72 641 9817.
E-mail address: tsunoda@nibio.go.jp (S.-i. Tsunoda).
[1] These authors contributed equally to this work.

0006-291X/$ - see front matter © 2009 Published by Elsevier Inc.
doi:10.1016/j.bbrc.2009.04.115

disease. For example, 4-1BBL, CD27L, CD30L, GITRL, LIGHT, OX40L, and TNF-α, which have costimulatory functions for survival, expansion, and effecter function of T cells, enhance systemic immunity to co-administered antigens [8]. There is, however, no comparative study to investigate the potential of TNF superfamily cytokines as mucosal vaccine adjuvants.

In this study, to develop effective and safe cytokine-based mucosal vaccine adjuvants, we compared the potential of TNF superfamily cytokines. We showed that intranasal coadministration of APRIL, TL1A, or TNF-α along with antigen induced strong antigen-specific systemic IgG and mucosal IgA antibody responses. In particular, TL1A induced the strongest immune responses at mucosal sites among TNF superfamily cytokines. These data suggest that TL1A is an attractive prototype for a mucosal vaccine adjuvant. This study is the first report to clearly demonstrate the potential of TNF superfamily cytokines as mucosal adjuvants. To develop a mucosal vaccine adjuvant, a pool of such information would be of great benefit.

Materials and methods

Adjuvants. Cholera toxin B subunit (CTB) was purchased from List Biological Laboratories (Campbell, CA). Sixteen types of recombinant TNF superfamily cytokines included human APRIL (18.6 kDa), mouse BAFF (23.2 kDa), mouse 4-1BBL (25.7 kDa), mouse CD27L (19.2 kDa), mouse CD30L (22 kDa), mouse CD40L (25 kDa), mouse EDA (23 kDa), mouse GITRL (16 kDa), mouse LIGHT (21 kDa), mouse LT-α (18.5 kDa), mouse OX40L (18 kDa), mouse TL1A (20 kDa), mouse TNF-α (17.5 kDa), mouse TRIAL (20 kDa), mouse TRANCS (36 kDa), mouse TWEAK (17 kDa) were purchased from R&D Systems (Minneapolis, MN).

Mice and immunization protocols. Female BALB/c mice were purchased from SLC (Hamamatsu, Japan) and used at 6 weeks of age. All of the animal experimental procedures in this study were performed in accordance with the National Institute of Biomedical Innovation guidelines for the welfare of animals. Mice were intranasally immunized with 100 μg of ovalbumin (OVA; Sigma Chemical Co., St. Louis, MO) and 1 μg CTB or each TNF superfamily cytokine included human APRIL (5.4×10^{-11} M/mouse), mouse BAFF (4.3×10^{-11} M/mouse), mouse 4-1BBL (3.9×10^{-11} M/mouse), mouse CD27L (5.2×10^{-11} M/mouse), mouse CD30L (4.5×10^{-11} M/mouse), mouse CD40L (4.0×10^{-11} M/mouse), mouse EDA (4.3×10^{-11} M/mouse), mouse GITRL (6.3×10^{-11} M/mouse), mouse LIGHT (4.8×10^{-11} M/mouse), mouse LT-α (5.4×10^{-11} M/mouse), mouse OX40L (5.6×10^{-11} M/mouse), mouse TL1A (5.0×10^{-11} M/mouse), mouse TNF-α (5.7×10^{-11} M/mouse), mouse TRAIL (5.0×10^{-11} M/mouse), mouse TRANCE (2.8×10^{-11} M/mouse), mouse TWEAK (5.9×10^{-11} M/mouse) in a total volume of 20 μl per mouse (10 μl/nostril). Mice were intranasally treated with OVA plus each of the TNF superfamily cytokines three times at weekly intervals.

Sample collection. Seven days after the final immunization, plasma and mucosal secretions (nasal washes, vaginal washes, and fecal extracts) were collected to assess antigen-specific IgG and IgA responses. Nasal and vaginal washes were collected by gently flushing the nasal passage or vaginal canal with 200 or 100 μl of sterile PBS, respectively. Fecal pellets (100 mg) were suspended in 1 ml of PBS and then vortexed for 30 min. The samples were centrifuged at 15,000g for 20 min, and then the supernatants were collected as fecal extracts.

Detection of antigen-specific antibody responses by ELISA. Antigen-specific IgG and IgA levels in plasma, nasal washes, vaginal washes, and fecal extracts were determined by ELISA. ELISA plates (Maxisorp, type 96F; Nalge Nunc International, Tokyo, Japan) were coated with 10 μg/ml OVA in 0.1 M carbonate buffer, respectively, and incubated overnight at 4 °C. The plates were incubated with blocking solution (Block Ace; Dainippon Sumitomo Pharmaceuticals, Osaka, Japan) at 37 °C for 2 h, and serum (1/500) or mucosal secretion dilutions (1/50) were added to the OVA-coated plates. After incubation at 37 °C for 2 h, the coated plates were washed with PBS–Tween 20 and incubated with the horse horseradish peroxidase-conjugated goat anti-mouse IgG solution or a biotin-conjugated goat anti-mouse IgA detection antibody (Southern Biotechnology Associates, Birmingham, AL) solution at 37 °C for 2 h, respectively. For detection of IgA, the plates were washed with PBS–Tween 20 and then incubated with the horseradish peroxidase-coupled streptavidin (Zymed Laboratories South San Francisco) for 1 h at rt. After incubation, the color reaction was developed with tetramethylbenzidine (MOSS, Inc., Pasadena, MD), stopped with 2 N H_2SO_4, and measured by $OD_{450-655}$ on a micro plate reader.

Isolation of splenocytes. Spleens were aseptically removed and placed in RPMI 1640 (Wako Pure Chemical Industries, Osaka, Japan) supplemented with 10% FBS, 50 μM 2-mercaptoethanol, and 1% antibiotic cocktail (Nacalai Tesque, Kyoto, Japan). Single-cell suspension of splenocytes was treated with ammonium chloride to lyse the red blood cells; they were then washed, counted, and suspended in RPMI supplemented with 10% FBS, 50 μM 2-mercaptoethanol, 1% antibiotic cocktail, non-essential amino acids solution, 1 mM sodium pyruvate, and 10 mM Hepes to a final concentration of 1×10^7 cells/ml.

Antigen-specific cytokine responses. Antigen-specific cytokine responses were evaluated using culturing splenocytes (5×10^6 cells/well) stimulated with OVA (1 mg/ml) *in vitro*. Cells were incubated at 37 °C for 72 h. Culture supernatants from *in vitro* unstimulated and OVA-stimulated cells were analyzed by the Bio-Plex Multiplex Cytokine Assay (Bio-Rad Laboratories, Hercules, CA) according to the manufacturer's instructions. The assay was read on a Luminex 100 (Austin, TX), and analyzed using the Bio-Plex Manager software. The mean concentration of cytokines in supernatants from OVA-stimulated cells over the unstimulated background was calculated.

Statistical analysis. All results are expressed as means ± SEM. Differences were compared using Bonferroni's method after analysis of variance (ANOVA).

Results and discussion

Development of novel mucosal vaccine adjuvants with high efficacy and safety has been expected. Among various adjuvant candidates, cytokines might be promising safe adjuvants because they are human-derived and able to enhance the primary and memory immune responses sufficiently to protect from various infections. In this study, we examined the potential of TNF superfamily cytokines as mucosal vaccine adjuvants.

In this study, we used 16 different TNF superfamily cytokines (APRIL, BAFF, 4-1BBL, CD27L, CD30L, CD40L, EDA, GITRL, LIGHT, LT-α, OX40L, TL1A, TNF-α, TRAIL, TRANCE, and TWEAK). To examine TNF superfamily cytokines' potential as mucosal adjuvants, the mice were intranasally immunized with 100 μg OVA plus each TNF superfamily cytokine (1 μg/mice) three times at weekly intervals. Seven days after the last immunization, we examined the level of anti-OVA IgG responses in serum by ELISA (Fig. 1A). As a result, intranasal immunization with OVA plus TL1A exhibited significantly higher OVA-specific IgG responses in serum than those immunized with OVA alone. OVA-specific IgG level of TL1A immunized mice was of similar magnitude to that induced by CTB, one of the most effective mucosal adjuvants. In addition, intranasal immunization with OVA plus APRIL or TNF-α also showed strong OVA-specific IgG responses in serum.

Murine serum IgG subclass responses have been used to assess the type of immune responses elicited by immunization with IgG1 indicative of Th2-type responses and IgG2a indicative of Th1-type responses. To assess the type of immune response induced by TNF superfamily cytokines, IgG subclass studies were also examined (Fig. 1B and C). As a result, OVA-specific IgG1 was significantly high in mice immunized with OVA plus TL1A and TNF-α, which are as strong as CTB. Mice immunized with OVA plus APRIL also tend to show strong OVA-specific IgG1 responses. On the other hand, APRIL showed the highest OVA-specific IgG2a responses as well as CTB. These results indicated that APRIL, TL1A, and TNF-α could induce strong immune responses via nasal administration and also induce an antigen-specific Th2-type immune response.

Next, in order to identify the characteristics of TNF superfamily cytokines as mucosal adjuvants, we examined the OVA-specific IgA responses in nasal washes from immunized mice as well as vaginal washes and fecal extracts, which are not administration sites (Fig. 2). In nasal washes, OVA-specific IgA level of TL1A immunized mice were significantly higher than OVA alone immunized mice, and this magnitude was similar to that induced by CTB (Fig. 2A). Mice immunized with OVA plus APRIL or TNF-α also tended to show strong OVA-specific IgA responses. In vaginal washes and fecal extracts, TL1A and TNF-α showed the highest OVA-specific IgA responses among TNF superfamily cytokines, while these magnitudes were lower than those immunized with OVA plus CTB (Fig. 2B and C). These results indicate that nasal immunization

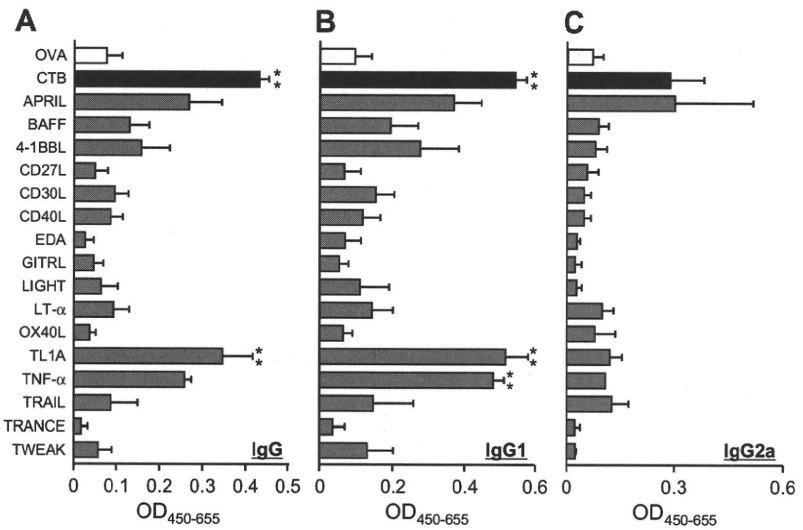

Fig. 1. Serum OVA-specific IgG responses by nasal immunization with OVA plus TNF superfamily cytokines. BALB/c mice were intranasally immunized with OVA alone, OVA plus CTB, or OVA plus each TNF superfamily cytokine three times at weekly intervals. Serum was collected 7 days after the last immunization and analyzed by ELISA for OVA-specific (A) total IgG, (B) IgG1, and (C) IgG2a responses at a 500-fold serum dilution. Data are presented as means ± SEM ($n = 5$; $^{**}P < 0.01$ versus value for OVA alone treated group by ANOVA).

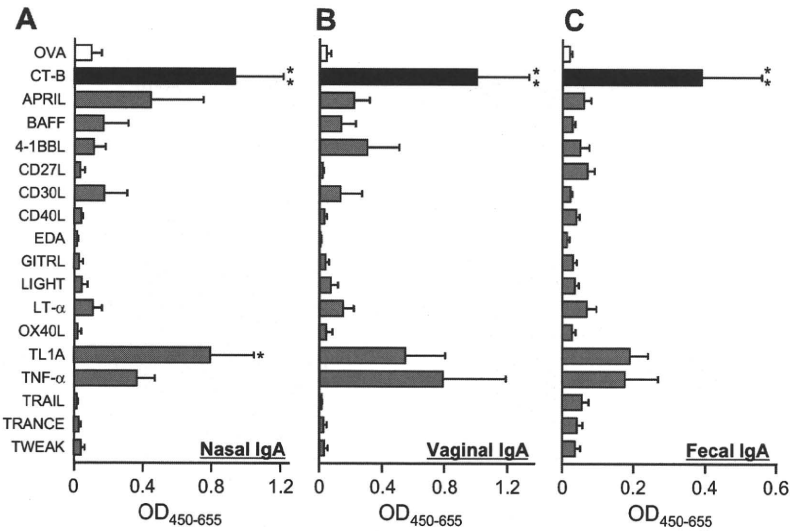

Fig. 2. OVA-specific mucosal IgA responses by nasal immunization with OVA plus TNF superfamily cytokines. BALB/c mice were intranasally immunized with OVA alone, OVA plus CTB, or OVA plus each TNF superfamily cytokines once a week for 3 weeks. Mucosal secretions were collected 7 days following the last immunization and then OVA-specific IgA responses in (A) nasal wash, (B) vaginal wash and (C) fecal extract were determined by ELISA. Data are presented as means ± SEM ($n = 5$; $^{*}P < 0.05$, $^{**}P < 0.01$ versus value for OVA alone treated group by ANOVA).

with TL1A effectively induced both antigen-specific systemic and mucosal immune responses, and indicated that TL1A might be a new candidate for mucosal vaccine adjuvants replacing toxin-based adjuvants. Among these cytokines, CD40–CD40L interaction is also known to play an important role in the generation of antigen-specific IgA positive B cells, and mount specific IgA responses to orally or parenterally administered antigens [9,10]. Indeed, Ninomiya et al. showed that intranasal administration of anti-CD40 antibody with antigens from the influenza virus induced protective immunity against influenza virus [11]. Our results showed that intranasal administration of CD40L could not enhance mucosal immunity against antigens, but the precise reason of these controversial results was unknown.

To clarify the mechanisms of immune response by each TNF superfamily cytokine, the release profiles of cytokines from splenocytes of immunized mice were analyzed. Culture supernatants from OVA-stimulated splenocytes collected from immunized mice were assessed for Th2-type cytokines IL-4 (Fig. 3A) and IL-5 (Fig. 3B) and Th1-type cytokines interferon-γ (IFNγ) (Fig. 3C) and TNF-α (Fig. 3D), using a multiplexed immunobeads assay. Splenocytes from mice immunized with OVA plus APRIL, TNF-α, or TL1A exhibited higher levels of Th2-type cytokines (IL-4 and IL-5) than those responses induced by OVA alone (Fig. 3A and B). In contrast, there was little difference in Th1-type cytokine (IFN-γ and TNF-α) secretion in all types of immunized mice (Fig. 3C and D). These results suggest that APRIL, TNF-α, and TL1A induced more strongly polarized Th2-type immune responses when used as mucosal vaccine adjuvants.

Our results indicate that TL1A induced the strongest mucosal immunity among the TNF superfamily cytokines. This is the first report to demonstrate TL1A mucosal adjuvant activity, induced antigen-specific systemic and mucosal immune responses in mice. The most recently identified member of the TNF superfamily, TL1A, is known to bind only to death receptor (DR) 3 expressed primarily on activated lymphocytes [12]. TL1A is also expressed on endothelial cells, normal lymphocytes, plasma cells, monocytes, and dendritic cells (DCs) [13,14]. TL1A can induce IFN-γ production of IL-12 and IL-18 primed T cells, whereas TL1A does not enhance IL-4 production from Th2 cells by systemic injection [15,16]. Therefore, it was believed that the TL1A/DR3 pathway played a dominant role in the Th1-type immune response by mucosal T cells in the inflamed mucosal site. On the other hand, a recent study showed that TL1A may act as soluble mediator or as cell-bound ligand to trigger DR3 on NKT and T cells, and this pair appears to provide an early signal for Th2-type cytokine production such as IL-4 and IL-13 [17]. We showed that the OVA-specific immune response of TL1A immunized mice was characterized by high levels of serum IgG1 and increased production of IL-4 and IL-5 from splenocytes of

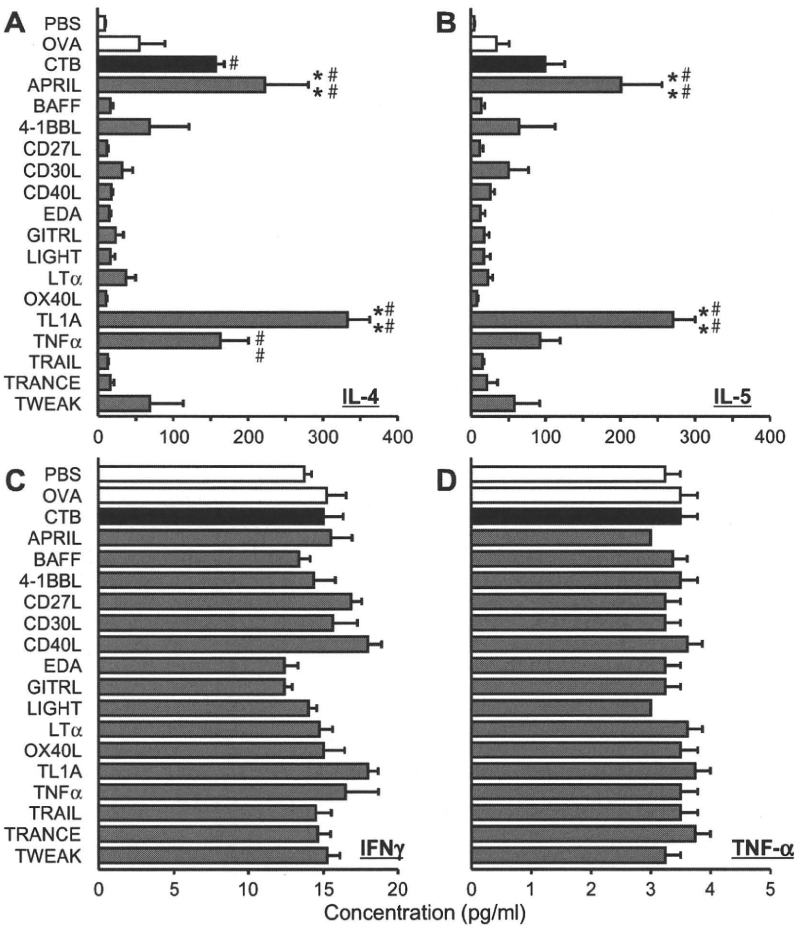

Fig. 3. Cytokine responses induced by nasal immunization with OVA plus adjuvants. BALB/c mice were intranasally immunized with OVA alone, OVA plus CTB, OVA plus each TNF superfamily cytokine three times at weekly intervals. Seven days after the last immunization, splenocytes from each group were cultured with 1 mg/ml OVA. Culture supernatants were harvested after 3 days of incubation, and then OVA-specific (A) IL-4, (B) IL-5, (C) IFNγ, and (D) TNF-α productions in culture supernatant were analyzed using the Bio-Plex Multiplex Cytokine Assay. Data are presented as means ± SEM ($n = 4$; $^{\#}P < 0.05$, $^{\#\#}P < 0.01$ versus value for PBS treated group by ANOVA; $^{**}P < 0.01$ versus value for OVA alone treated group by ANOVA).

immunized mice, suggesting a Th2-type immune response. The administration route of antigen immunization might be critical for influencing the type of immune response, although the precise reason for these contradictory results remains unclear. We are currently examining the mechanism of TL1A-induced Th2-type immune responses in more detail. In addition, the potential of TL1A as a mucosal vaccine adjuvant should be enhanced because the strength of immune responses by TL1A was lower than that of CTB. We have developed a novel technology to produce mutant cytokines using phage display [18–21]. We previously produced a bioactive mutant TNF-α with 6-fold stronger *in vitro* bioactivity and 13-fold stronger *in vivo* bioactivity compared with wild-type TNF-α [20]. We are now attempting to generate mutant TL1A with improved adjuvanticity.

We showed that APRIL and TNF-α also had the potential to function as a mucosal vaccine adjuvant, although the strength of immune responses in those immunized mice was lower than mice immunized with TL1A. The analysis of knockout mice suggested that APRIL would deliver B cell activation signals and induce IgA production against antigens from pathogenic microorganisms and viruses [22]. In addition, it was also reported that TNF-α played an important role in IgA production [23]. Future examination is needed to determine a more precise mechanism of IgA production by APRIL and TNF-α.

Regulation of Th1- and Th2-type immune responses is the major goal for the development of mucosal vaccines because these types of immune responses would control protective immunity against viral and bacterial infections by maximizing antigen-specific antibodies and CTL responses [1,3]. To induce both antigen-specific antibodies and CTL responses, combinatorial administration of TL1A with another mucosal adjuvant, which can induce Th1-type immune responses, is applicable. We have already screened the other cytokines and succeeded in finding candidates that can effectively induce CTL responses at the mucosal site. The combinatorial effect of the cytokines and TL1A as a mucosal vaccine adjuvant is now under examination.

In summary, our study showed that TL1A induced two layers of protective immunity when administered intranasally with a vaccine antigen. Our results indicate that TL1A is an effective mucosal adjuvant.

Acknowledgments

The authors declare no conflict of interests. This study was supported in part by Grants-in-Aid for Scientific Research from the Ministry of Education, Culture, Sports, Science and Technology of Japan (MEXT) and Japan Society for the Promotion of Science (JSPS), by grants from the Ministry of Health, Labor, and Welfare in Japan and from the Japan Health Sciences Foundation and by the grant from Takeda Science Foundation.

References

[1] K. Eriksson, J. Holmgren, Recent advances in mucosal vaccines and adjuvants, Curr. Opin. Immunol. 14 (2002) 666–672.
[2] B.F. Haynes, R.J. Shattock, Critical issues in mucosal immunity for HIV-1 vaccine development, J. Allergy Clin. Immunol. 122 (2008) 3–9. quiz 10–11.
[3] J. Holmgren, C. Czerkinsky, Mucosal immunity and vaccines, Nat. Med. 11 (2005) S45–S53.
[4] S.L. Gorbach, C.M. Khurana, Toxigenic *Escherichia coli* in infantile diarrhea in Chicago, J. Lab. Clin. Med. 78 (1971) 981–982.
[5] M. Mutsch, W. Zhou, P. Rhodes, M. Bopp, R.T. Chen, T. Linder, C. Spyr, R. Steffen, Use of the inactivated intranasal influenza vaccine and the risk of Bell's palsy in Switzerland, N. Engl. J. Med. 350 (2004) 896–903.
[6] Y. Collette, A. Gilles, P. Pontarotti, D. Olive, A co-evolution perspective of the TNFSF and TNFRSF families in the immune system, Trends Immunol. 24 (2003) 387–394.
[7] T. Hehlgans, K. Pfeffer, The intriguing biology of the tumour necrosis factor/tumour necrosis factor receptor superfamily: players, rules and the games, Immunology 115 (2005) 1–20.
[8] K. Tamada, L. Chen, Renewed interest in cancer immunotherapy with the tumor necrosis factor superfamily molecules, Cancer Immunol. Immunother. 55 (2006) 355–362.
[9] T. Kawabe, T. Naka, K. Yoshida, T. Tanaka, H. Fujiwara, S. Suematsu, N. Yoshida, T. Kishimoto, H. Kikutani, The immune responses in CD40-deficient mice: impaired immunoglobulin class switching and germinal center formation, Immunity 1 (1994) 167–178.
[10] P. Bergqvist, E. Gardby, A. Stensson, M. Bemark, N.Y. Lycke, Gut IgA class switch recombination in the absence of CD40 does not occur in the lamina propria and is independent of germinal centers, J. Immunol. 177 (2006) 7772–7783.
[11] A. Ninomiya, K. Ogasawara, K. Kajino, A. Takada, H. Kida, Intranasal administration of a synthetic peptide vaccine encapsulated in liposome together with an anti-CD40 antibody induces protective immunity against influenza A virus in mice, Vaccine 20 (2002) 3123–3129.
[12] T.S. Migone, J. Zhang, X. Luo, L. Zhuang, C. Chen, B. Hu, J.S. Hong, J.W. Perry, S.F. Chen, J.X. Zhou, Y.H. Cho, S. Ullrich, P. Kanakaraj, J. Carrell, E. Boyd, H.S. Olsen, G. Hu, L. Pukac, D. Liu, J. Ni, S. Kim, R. Gentz, P. Feng, P.A. Moore, S.M. Ruben, P. Wei, TL1A is a TNF-like ligand for DR3 and TR6/DcR3 and functions as a T cell costimulator, Immunity 16 (2002) 479–492.
[13] G. Bamias, M. Mishina, M. Nyce, W.G. Ross, G. Kollias, J. Rivera-Nieves, T.T. Pizarro, F. Cominelli, Role of TL1A and its receptor DR3 in two models of chronic murine ileitis, Proc. Natl. Acad. Sci. USA 103 (2006) 8441–8446.
[14] J.L. Prehn, L.S. Thomas, C.J. Landers, Q.T. Yu, K.S. Michelsen, S.R. Targan, The T cell costimulator TL1A is induced by FcgammaR signaling in human monocytes and dendritic cells, J. Immunol. 178 (2007) 4033–4038.
[15] J.L. Prehn, S. Mehdizadeh, C.J. Landers, X. Luo, S.C. Cha, P. Wei, S.R. Targan, Potential role for TL1A, the new TNF-family member and potent costimulator of IFN-gamma, in mucosal inflammation, Clin. Immunol. 112 (2004) 66–77.
[16] K.A. Papadakis, D. Zhu, J.L. Prehn, C. Landers, A. Avanesyan, G. Lafkas, S.R. Targan, Dominant role for TL1A/DR3 pathway in IL-12 plus IL-18-induced IFN-gamma production by peripheral blood and mucosal CCR9+ T lymphocytes, J. Immunol. 174 (2005) 4985–4990.
[17] L. Fang, B. Adkins, V. Deyev, E.R. Podack, Essential role of TNF receptor superfamily 25 (TNFRSF25) in the development of allergic lung inflammation, J. Exp. Med. 205 (2008) 1037–1048.
[18] Y. Yamamoto, Y. Tsutsumi, Y. Yoshioka, T. Nishibata, K. Kobayashi, T. Okamoto, Y. Mukai, T. Shimizu, S. Nakagawa, S. Nagata, T. Mayumi, Site-specific PEGylation of a lysine-deficient TNF-alpha with full bioactivity, Nat. Biotechnol. 21 (2003) 546–552.
[19] Y. Yoshioka, Y. Tsutsumi, S. Ikemizu, Y. Yamamoto, H. Shibata, T. Nishibata, Y. Mukai, T. Okamoto, M. Taniai, M. Kawamura, Y. Abe, S. Nakagawa, S. Nagata, Y. Yamagata, T. Mayumi, Optimal site-specific PEGylation of mutant TNF-alpha improves its antitumor potency, Biochem. Biophys. Res. Commun. 315 (2004) 808–814.
[20] H. Shibata, Y. Yoshioka, S. Ikemizu, K. Kobayashi, Y. Yamamoto, Y. Mukai, T. Okamoto, M. Taniai, M. Kawamura, Y. Abe, S. Nakagawa, T. Hayakawa, S. Nagata, Y. Yamagata, T. Mayumi, H. Kamada, Y. Tsutsumi, Functionalization of tumor necrosis factor-alpha using phage display technique and PEGylation improves its antitumor therapeutic window, Clin. Cancer Res. 10 (2004) 8293–8300.
[21] H. Shibata, Y. Yoshioka, A. Ohkawa, K. Minowa, Y. Mukai, Y. Abe, M. Taniai, T. Nomura, H. Kayamuro, H. Nabeshi, T. Sugita, S. Imai, K. Nagano, T. Yoshikawa, T. Fujita, S. Nakagawa, A. Yamamoto, T. Ohta, T. Hayakawa, T. Mayumi, P. Vandenabeele, B.B. Aggarwal, T. Nakamura, Y. Yamagata, S. Tsunoda, H. Kamada, Y. Tsutsumi, Creation and X-ray structure analysis of the tumor necrosis factor receptor-1-selective mutant of a tumor necrosis factor-alpha antagonist, J. Biol. Chem. 283 (2008) 998–1007.
[22] E. Castigli, S. Scott, F. Dedeoglu, P. Bryce, H. Jabara, A.K. Bhan, E. Mizoguchi, R.S. Geha, Impaired IgA class switching in APRIL-deficient mice, Proc. Natl. Acad. Sci. USA 101 (2004) 3903–3908.
[23] H. Tezuka, Y. Abe, M. Iwata, H. Takeuchi, H. Ishikawa, M. Matsushita, T. Shiohara, S. Akira, T. Ohteki, Regulation of IgA production by naturally occurring TNF/iNOS-producing dendritic cells, Nature 448 (2007) 929–933.

Biomaterials 30 (2009) 5869–5876

Contents lists available at ScienceDirect

Biomaterials

journal homepage: www.elsevier.com/locate/biomaterials

The use of a mutant TNF-α as a vaccine adjuvant for the induction of mucosal immune responses

Hiroyuki Kayamuro [a,b,1], Yasuhiro Abe [a,1], Yasuo Yoshioka [a,c,1], Kazufumi Katayama [b,d], Tetsuya Nomura [a,b], Tokuyuki Yoshida [a,b], Kohei Yamashita [a,b], Tomoaki Yoshikawa [a,b], Yuichi Kawai [e], Tadanori Mayumi [e], Takachika Hiroi [d], Norio Itoh [b], Kazuya Nagano [a], Haruhiko Kamada [a,c], Shin-ichi Tsunoda [a,c,*], Yasuo Tsutsumi [a,b,c]

[a] Laboratory of Pharmaceutical Proteomics, National Institute of Biomedical Innovation (NiBio), 7-6-8 Saito-Asagi, Ibaraki, Osaka 567-0085, Japan
[b] Graduate School of Pharmaceutical Sciences, Osaka University, 1-6, Yamadaoka, Suita, Osaka 565-0871, Japan
[c] The Center for Advanced Medical Engineering and Informatics, Osaka University, 1-6, Yamadaoka, Suita, Osaka 565-0871, Japan
[d] Department of Allergy and Immunology, The Tokyo Metropolitan Institute of Medical Science, 3-18-22, Honkomagome, Bunkyo-ku, Tokyo 113-8613, Japan
[e] Faculty of Pharmaceutical Sciences, Kobe-Gakuin University, 1-1-3, Minatojima, Chuo-ku, Kobe 650-8586, Japan

ARTICLE INFO

Article history:
Received 19 May 2009
Accepted 6 July 2009
Available online 30 July 2009

Keywords:
Bioactivity
Cytokine
Mucosa
Immunomodulation

ABSTRACT

Safe and potent adjuvants are required in order to establish effective mucosal vaccines. Cytokines are promising adjuvants because they are human-derived safe biomaterial and display immune-modulating functions. We have created a mutant tumor necrosis factor-α (TNF-α), mTNF-K90R, that exhibits high bioactivity and resistance to proteases. Here, we examined the potential of mTNF-K90R as a mucosal adjuvant. Initially, we showed that intranasal co-administration of mTNF-K90R with ovalbumin (OVA) potently produced OVA-specific Immunoglobulin (Ig) G antibodies (Abs) in serum and IgA Abs both at local and distal mucosal sites compared to co-administration with wild-type TNF-α. The OVA-specific immune response was characterized by high levels of serum IgG1 and increased production of interleukin-4 (IL-4), IL-5 and IL-10 from splenocytes of immunized mice, suggesting a Th2 response. Furthermore, intranasal immunization with an antigen from influenza virus plus mTNF-K90R exhibited mucosal adjuvant activity for induction of both systemic and mucosal immune responses. Importantly, histopathological examination of the nasal tissue of mTNF-K90R treated mice detected no signs of toxicity. These findings suggest that mTNF-K90R is safe and effective mucosal adjuvant and this system may have potential application as a universal mucosal adjuvant system for mucosal vaccines improving the immune response to a variety of viral antigens.

1. Introduction

Mucosal immunity forms the first line of defense against various infectious diseases. The majority of emerging and re-emerging pathogens, including *Vibrio cholerae*, pathogenic *Escherichia coli*, HIV or influenza virus, invade and infect *via* the mucosal surfaces of the host gastrointestinal, respiratory and/or genitourinary tracts [1,2]. An important aspect of the immune response at mucosal surfaces is the production of polymeric immunoglobulin (Ig) A antibodies (Abs), as well as their transport across the epithelium and release as secretory IgA [3]. Because this IgA response represents the major mechanism for defense against viral and bacterial infections, recent efforts have been focused on the development of vaccines that are capable of inducing IgA production as well as cytotoxic T cell activation efficiently in mucosal tissues.

Mucosal vaccines administered either orally or nasally have been shown to be effective in inducing antigen-specific immune responses at both systemic and mucosal compartments [4,5]. Because of this two-layered protective immunity, mucosal vaccines are thought to be an ideal strategy for combating both emerging and re-emerging infectious diseases. However the mucosal antigen-specific immune response is weak because most protein antigens, such as non-living macromolecules or protein-subunit antigens, can evoke only a weak or undetectable adaptive immune response when they are applied mucosally [6]. Therefore, one strategy to overcome the weakness of the immune response is a co-administration of mucosal adjuvant

* Corresponding author. Laboratory of Pharmaceutical Proteomics, National Institute of Biomedical Innovation (NiBio), 7-6-8 Saito-Asagi, Ibaraki, Osaka 567-0085, Japan. Tel.: +81 72 641 9811; fax: +81 72 641 9817.
E-mail address: tsunoda@nibio.go.jp (S.-i. Tsunoda).
[1] These authors contributed equally to the work.

0142-9612/$ – see front matter © 2009 Elsevier Ltd. All rights reserved.
doi:10.1016/j.biomaterials.2009.07.009

with the vaccine antigen [4]. Unfortunately, the development of safe and effective mucosal adjuvant has proved to be challenging. As a potent mucosal vaccine adjuvant, cholera toxin (CT) or heat liable toxin have been used in experimental studies. However, the watery diarrhea induced by the administration of these toxins precludes their use as oral adjuvants in humans [7]. In addition, recent reports show that a human vaccine containing inactivated influenza and heat liable toxin as a mucosal adjuvant results in a very high incidence of Bell's palsy [8]. Therefore, development of novel mucosal vaccine adjuvants with high efficacy and safety is urgently required for clinical applications.

Cytokines are promising candidate adjuvants because they are human-derived and able to enhance the primary and memory immune responses sufficiently for protection against various infections [9–11]. One of the most important cytokines of adaptive and innate immune response is tumor necrosis factor-α (TNF-α), a proinflammatory cytokine primarily produced by T cells and macrophages [12]. TNF-α has been reported to affect certain phases of the immune process, including innate immune activation, dendritic cells (DC) maturation/recruitment, T cell activation, or pathogen clearance [13]. Indeed many reports have shown that TNF-α exerts adjuvant activities against viral infection in various model systems [14–16]. Therefore the application of TNF-α in the development of a vaccine adjuvant has been anticipated for some time. However the application of TNF-α as a mucosal vaccine adjuvant has not been reported because TNF-α administered by mucosal routes is rapidly degraded at the mucosal surface. Therefore, the maximum adjuvant effects of TNF-α are quite limited in the mucosal environment.

Previously, we have produced a bioactive lysine-deficient mutant TNF-αs from a phage library expressing mutant TNF-αs in which all of the lysine residues that act as a site of trypsin-type protease recognition were replaced with other amino acids [17–19]. Lysine-deficient mutant TNF-αs were more resistant to proteolytic cleavage than wild-type TNF-α (wTNF-α) due to the lack of lysine residues. Furthermore we demonstrated that the mTNF-K90R, one of the lysine-deficient mutant TNF-αs, showed 6-fold stronger *in vitro* bioactivity and 13-fold stronger *in vivo* bioactivity compared with wTNF-α [18].

In this study, to develop effective and safe cytokine-based mucosal vaccine adjuvants, we examined the potential of mTNF-K90R as a nasal vaccine adjuvant. We demonstrate that intranasal administration of vaccine antigen with mTNF-K90R as an adjuvant induces a strong antigen-specific systemic IgG and mucosal IgA response. In addition, the safety of mTNF-K90R was confirmed by pathological examination. These results suggest that mTNF-K90R is an attractive mucosal vaccine adjuvant for clinical application.

2. Materials and methods

2.1. Recombinant TNF-αs

wTNF-α and mTNF-K90R were prepared in house as described previously [18]. Endotoxin level was quantified using a Limulus amebocyte lysate assay kit (QCL-1000, BioWhittaker, Walkersville, MD). The endotoxin content of purified TNF-α and its mutant was <0.02 EU μg^{-1} protein.

2.2. Mice and immunization protocols

Female BALB/c mice were purchased from Nippon SLC (Kyoto, Japan) and used at 6–8 weeks of age. All of the animal experimental procedures were performed in accordance with the institutional ethical guidelines for animal experiments. Mice were intranasally immunized with a 20 μl aliquot (10 μl per nostril) containing 100 μg of ovalbumin (OVA; Sigma Chemical Co., St. Louis, MO) as antigen and 1 or 5 μg of wTNF-α or mTNF-K90R on days 0, 7 and 14. As positive control, mice were intranasally immunized with the same volume containing 100 μg of OVA and 1 μg cholera toxin B subunit (CTB; List Biological Laboratories, Campbell, CA) on days 0, 7 and 14. In the influenza virus studies, 1 μg baculovirus-expressed recombinant hemagglutinin (HA) derived from New Cal/99 virus (Protein Sciences, Meriden, CT), was immunized with 1 μg CTB or 5 μg mTNF-K90R on days 0, 7 and 14.

2.3. Sample collection

One week after the final immunization, plasma and mucosal secretions (nasal washes, saliva, vaginal washes and fecal extracts) were collected to assess antigen-specific Ab responses. Nasal and vaginal washes were collected by gentle flushing of the nasal passage or vaginal canal with 200 μl or 100 μl of sterile phosphate buffered saline (PBS), respectively. Fecal pellets (100 mg) were suspended in 1 ml of PBS and then vortexed for 30 min. The samples were centrifuged at 15 000g for 20 min and the supernatants were then collected as fecal extracts. Secreted saliva was collected from mice intraperitoneally injected with 0.2 mg of pilocarpine–HCl (Wako Pure Chemical Industries, Osaka, Japan).

2.4. Detection of antigen-specific Ab responses by enzyme-linked immunosorbent assay (ELISA)

Antigen-specific Ab levels in plasma, nasal washes, saliva, vaginal washes and fecal extracts were determined by ELISA. ELISA plates (Maxisorp, type 96F; Nalge Nunc International, Tokyo, Japan) were coated with 10 μg ml^{-1} OVA or 2 μg ml^{-1} HA in 0.1 M carbonate buffer and incubated overnight at 4 °C. The plates were incubated with blocking solution (Block Ace; Dainippon Sumitomo Pharmaceuticals, Osaka, Japan) at 37 °C for 2 h, and serum or mucosal secretion dilutions were added to the antigen-coated plates. After incubation at 37 °C for 2 h, the coated plates were washed with PBS–Tween 20 and incubated with a horseradish peroxidase-conjugated goat anti-mouse IgG solution or a biotin-conjugated goat anti-mouse IgA detection Ab (Southern Biotechnology Associates, Birmingham, AL) solution at 37 °C for 2 h, respectively. For detection of IgA, the plates were washed with PBS–Tween 20 and then incubated with the horseradish peroxidase-coupled streptavidin (Zymed Laboratories, South San Francisco, CA) for 1 h at RT. After incubation, the color reaction was developed with tetramethylbenzidine (MOSS, Inc. Pasadena, MD), stopped with 2 N H_2SO_4, and measured by $OD_{450-655}$ on a microplate reader.

2.5. Isolation of splenocytes

Spleens were aseptically removed and placed in RPMI 1640 (Wako Pure Chemical Industries, Osaka, Japan) supplemented with 10% fetal bovine serum, 50 μM 2-mercaptoethanol and 1% antibiotic cocktail (Nacalai tesque, Kyoto, Japan). Single-cell suspension of splenocytes was treated with ammonium chloride to lyse the red blood cells, washed, counted, and suspended in RPMI supplemented with 10% fetal bovine serum, 50 μM 2-mercaptoethanol, 1% antibiotic cocktail, 10 ml L^{-1} of a 100× nonessential amino acids solution (NEAA; Gibco-BRL), 1 mM sodium pyruvate, and 10 mM HEPES to a final concentration of 1×10^7 cells ml^{-1}.

2.6. Antigen-specific cytokine responses

Antigen-specific cytokine responses were evaluated by culturing the splenocytes (5×10^6 cells $well^{-1}$) stimulated with OVA (1 mg ml^{-1}) *in vitro*. Cells were incubated at 37 °C for 24 h (interferon-γ (IFN-γ) enzyme-linked immunospot (ELISPOT) assay), 48 h (IL-4 ELISPOT assay) or 72 h (multiplex cytokine assay).

2.7. Multiplex cytokine assay

Culture supernatants from *in vitro* unstimulated and OVA-stimulated cells were analyzed by the Bio-Plex Multiplex Cytokine Assay (Bio-Rad Laboratories, Hercules, CA) according to the manufacturer's instructions. The assay was read on a Luminex 100 (Austin, TX), and analyzed using Bio-Plex Manager software. The mean concentration of cytokines in supernatants from OVA-stimulated cells over the unstimulated background was then calculated.

2.8. Cytokine ELISPOT assay

An ELISPOT assay was performed to detect IFN-γ and IL-4 producing cells. After 24 h (IFN-γ) or 48 h (IL-4) incubation at 37 °C, the plate was washed, and the IFN-γ and IL-4 producing cells were measured by an ELISPOT assay kit (BD Biosciences), according to the manufacturer's instructions.

2.9. Fluorescence microscopy

BALB/c mice were administered intranasally with fluorescent isothiocyanate (FITC) labeled OVA (FITC-OVA; Molecular Probes–Invitrogen, Eugene, OR) at 50 μg $mouse^{-1}$ with or without mTNF-K90R (5 μg $mouse^{-1}$). After 15 min, the heads of the anesthetized mice were severed from the body. The heads were placed in fixative solution, and embedded in OCT compound (Sakura FineTek Japan Co. Ltd., Tokyo, Japan) and frozen tissue sections were prepared. FITC-OVA was observed under fluorescence microscopy (×20).

2.10. Histopathological analysis

For three times immunization protocol, BALB/c mice were immunized with OVA with or without mTNF-K90R at a dose of 1 μg, 5 μg or 25 μg on days 0, 7 and 14.

Seven days after the last immunization, heads of the mice were severed from the body and then placed in fixative solution (4% paraformaldehyde). Histopathological examination was performed by the Applied Medical Research Laboratory (Osaka, Japan). For single immunization protocol, BALB/c mice were immunized with OVA with or without mTNF-K90R at a dose of 5 μg. At 2 h after single immunization, histopathological examination was performed using the same protocol.

2.11. Statistical analysis

All results are expressed as mean ± SEM. Statistical significance in differences were evaluated by Newman–Keuls Multiple Comparison Test after analysis of variance (ANOVA).

3. Results

3.1. Mucosal adjuvant activity of mTNF-K90R

To examine the properties of mTNF-K90R as a mucosal vaccine adjuvant, mice were intranasally immunized with 100 μg OVA plus wTNF-α (1 μg mice^{-1}), mTNF-K90R (1 μg mice^{-1}, 5 μg mice^{-1}), or CTB (1 μg mice^{-1}) three times at weekly intervals. Seven days after the last immunization, we examined the level of anti-OVA Abs response in the serum by ELISA (Fig. 1A). Intranasal immunization with OVA plus 1 μg mTNF-K90R induced higher levels of anti-OVA IgG Ab response in serum than after immunization with OVA alone or OVA plus 1 μg wTNF-α. Furthermore, OVA-specific IgG Ab levels of mTNF-K90R immunized mice were of a similar magnitude to those immunized with CTB, a common laboratory mucosal adjuvant.

Serum IgG subclass responses have been used to assess the type of immune response elicited by immunization. For example, IgG1 is indicative of a Th2-type response whereas IgG2a is indicative of a Th1-type response. To assess the type of immune response induced by mTNF-K90R, serum OVA-specific IgG subclass responses were also examined (Fig. 1B). OVA-specific IgG1 Ab levels of 1 μg mTNF-K90R immunized mice were higher than those immunized with OVA alone or OVA plus 1 μg wTNF-α, and as well as in mice immunized with CTB. However, the level of OVA-specific IgG2a was low in all groups, indicating that mTNF-K90R may induce immune responses with an antigen-specific Th2 component.

Next, we examined the OVA-specific IgA secretion in nasal washes, vaginal washes, and fecal extracts from immunized mice (Fig. 2). As expected, immunization with OVA plus CTB induced strong anti-OVA IgA secretion in all mucosal tissues. Nasal immunization with OVA plus 1 μg of mTNF-K90R tended to induce high levels of OVA-specific IgA secretion in nasal tissue and fecal extract compared with after immunization with OVA plus 1 μg wTNF-α. The IgA level of 1 μg mTNF-K90R immunized mice in nasal tissue was of a similar magnitude to those immunized with CTB. In contrast, the IgA level in vaginal tissue and fecal extract was lower for the 1 μg mTNF-K90R treated mice compared with that of CTB treated mice. Nasal immunization with OVA plus 5 μg of mTNF-K90R induced high OVA-specific IgA secretion in multiple mucosal tissues compared to 1 μg of mTNF-K90R and comparable anti-OVA Abs responses to those induced with OVA plus CTB. These results indicate that mTNF-K90R is an attractive mucosal vaccine adjuvant for the induction of antigen-specific systemic IgG and mucosal IgA responses.

3.2. Antigen-specific cytokine responses of mTNF-K90R

To clarify the mechanism of immune response elicited by mTNF-K90R, the release profiles of cytokines from splenocytes of OVA-immunized mice were analyzed. Culture supernatants from

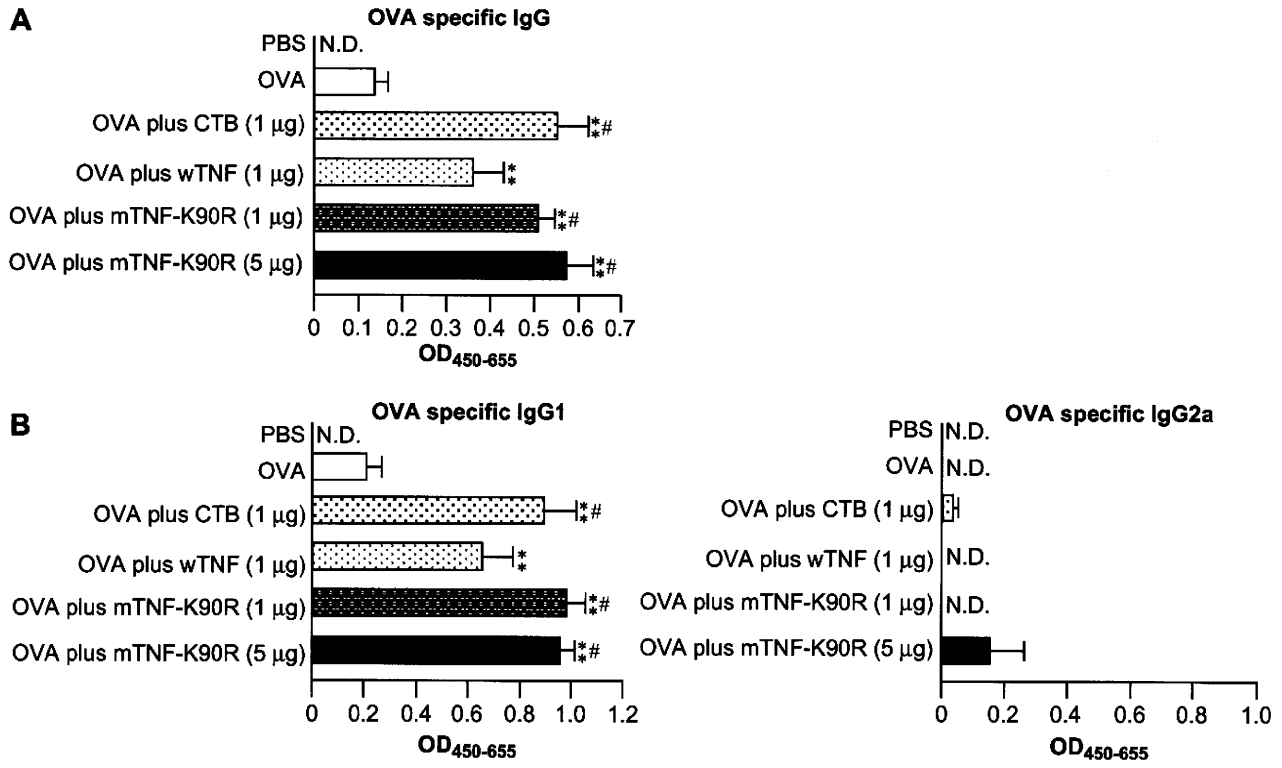

Fig. 1. Serum OVA-specific IgG Abs response after nasal immunization with OVA plus adjuvant. BALB/c mice were intranasally immunized with OVA alone, OVA plus 1 μg CTB, OVA plus 1 μg wTNF-α, OVA plus 1 μg mTNF-K90R or OVA plus 5 μg mTNF-K90R once a week for three consecutive weeks. Serum was collected 1 wk after the last immunization and analyzed by ELISA for OVA-specific IgG (A) and IgG subclass (B) at a 1:100 dilution of serum. Data represents the mean of absorbance 450 nm (reference wave, 655 nm). N.D; not detected. Data are presented as means ± SEM ($n = 7$; $^{**}P < 0.01$ *versus* value for OVA alone treated group by ANOVA; $^{\#}P < 0.05$ *versus* value for OVA plus wTNF-α treated group by ANOVA).

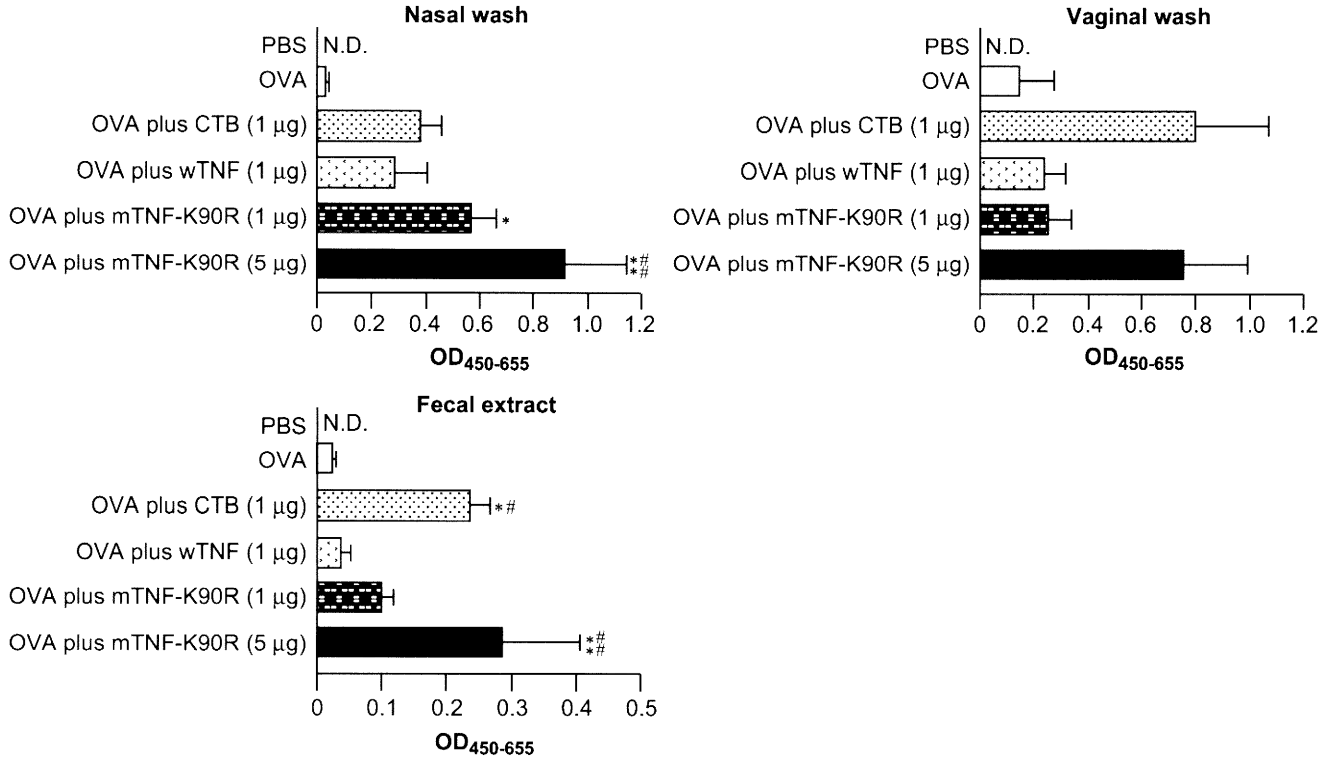

Fig. 2. OVA-specific mucosal IgA Abs response after nasal immunization with OVA plus adjuvant. BALB/c mice were intranasally immunized with OVA alone, OVA plus 1 μg CTB, OVA plus 1 μg wTNF-α, OVA plus 1 μg mTNF-K90R or OVA plus 5 μg mTNF-K90R once a week for three consecutive weeks. Mucosal secretions were collected 1 wk after the last immunization and OVA-specific IgA Abs responses in nasal wash, vaginal wash and fecal extract were determined by ELISA at a 1:8 dilution. Data represents the mean of absorbance 450 nm (reference wavelength, 655 nm). Data are presented as means ± SEM ($n = 7$; $^{*}P < 0.05$, $^{**}P < 0.01$ *versus* value for OVA alone treated group by ANOVA; $^{\#}P < 0.05$, $^{\#\#}P < 0.01$ *versus* value for OVA plus wTNF-α treated group by ANOVA).

OVA-stimulated splenocytes collected from immunized mice were assessed for Th2-type cytokines IL-4, IL-5, IL-10, granulocyte macrophage colony-stimulating factor (GM-CSF) (Fig. 3A) and Th1-type cytokines IL-12 and IFN-γ (Fig. 3B), using a multiplexed immunobeads assay. Splenocytes from mice immunized with OVA plus 1 μg mTNF-K90R exhibited higher levels of Th2-type cytokines (IL-4, IL-5, IL-10 and GM-CSF) than those responses induced with OVA plus 1 μg wTNF-α or CTB (Fig. 3A). In contrast, there was hardly any difference in Th1-type cytokine (IL-12 and IFN-γ) secretion amongst all of the immunized mice (Fig. 3B). To further characterize the type of immune response, the level of OVA-specific IFN-γ and IL-4-secreting splenocytes from OVA-immunized mice with the various adjuvants was determined using a cytokine-specific ELISPOT assay (Fig. 4). The level of OVA-specific IL-4-secreting splenocytes from OVA-immunized mice with mTNF-K90R was greater than those responses observed after administration of wTNF-α or CTB. By contrast, the level of IFN-γ-secreting splenocytes in OVA-immunized mice with mTNF-K90R was no different from the levels observed for mice immunized with OVA alone. These results suggested that mTNF-K90R induced a more strongly polarized Th2-type immune response when mTNF-K90R was used as a mucosal vaccine adjuvant.

3.3. Mucosal adjuvant efficacy against influenza virus

We anticipated that a mucosal influenza virus-neutralizing antibody response would generate an ideal vaccine against these infectious diseases. To estimate the mucosal adjuvant efficacy of mTNF-K90R for influenza virus HA vaccine, the antibody response against HA was examined in mice intranasally immunized with mTNF-K90R (Fig. 5). Mice receiving HA plus 5 μg of mTNF-K90R induced a significantly greater anti-HA IgG or IgA response in serum, saliva or nasal wash compared with mice receiving HA alone or HA plus CTB. These results indicated that application of mTNF-K90R as a nasal vaccine adjuvant to viral infectious diseases might be an effective strategy.

3.4. Localization of antigens into nasopharyngeal-associated lymphoreticular tissue (NALT)

Because NALT plays an important role in the initial induction of the mucosal immune response, it was important to determine the tissue localization of the antigens. To characterize the mechanism of mTNF-K90R in the induction of OVA-specific mucosal and systemic immune responses, we examined the localization of OVA in NALT derived from mice that were immunized with OVA in the absence or presence of mTNF-K90R (Fig. 6). Fluorescence microscopic analysis revealed that FITC-OVA was mainly located beneath the nasal epithelium surrounding NALT in mice treated with FITC-OVA alone. By contrast, in addition to the subepithelial region, FITC-OVA was also observed within NALT after co-administration of mTNF-K90R. These results indicate that mTNF-K90R might induce the effective entry of antigens into NALT due to increasing nasal epithelial permeability. We believe that the observed response of mTNF-K90R in the nasal epithelial reflects one of the mechanisms for the induction of antigen-specific mucosal and systemic immune response in mice.

3.5. Safety examination of mTNF-K90R

While enterotoxin-based adjuvants display a strong mucosal response, they also induce severe central nervous system damage

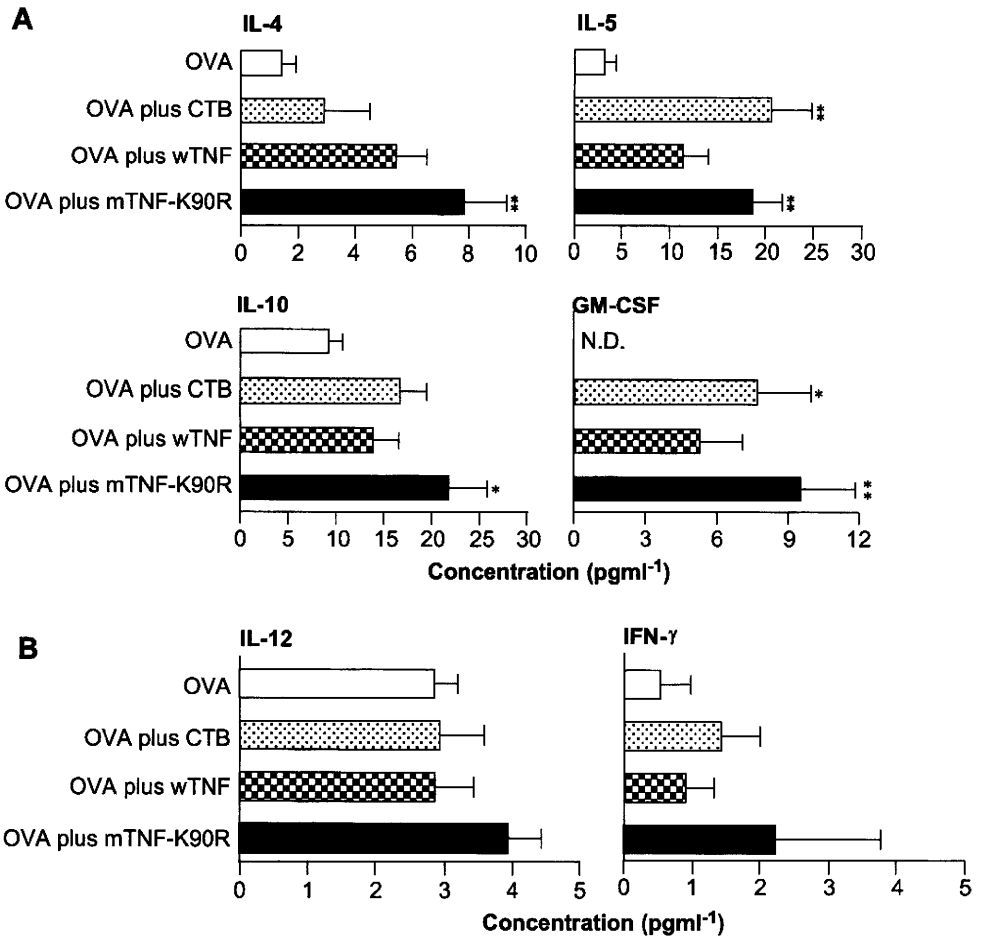

Fig. 3. Cytokine response induced after nasal immunization with OVA plus adjuvant. BALB/c mice were intranasally immunized with OVA alone, OVA plus 1 μg CTB, OVA plus 1 μg wTNF-α or OVA plus 1 μg mTNF-K90R once a week for three consecutive weeks. One week after the last immunization, splenocytes from each group were cultured with 1 mg ml^{-1} OVA. Culture supernatants were harvested following 3 days of incubation, and OVA-specific Th2-type (A) and Th1-type (B) cytokine productions in culture supernatant were analyzed by using the Bio-Plex Multiplex Cytokine Assay. Data are presented as means ± SEM ($n = 6$; $^{*}P < 0.05$, $^{**}P < 0.01$ *versus* value for OVA alone treated group by ANOVA).

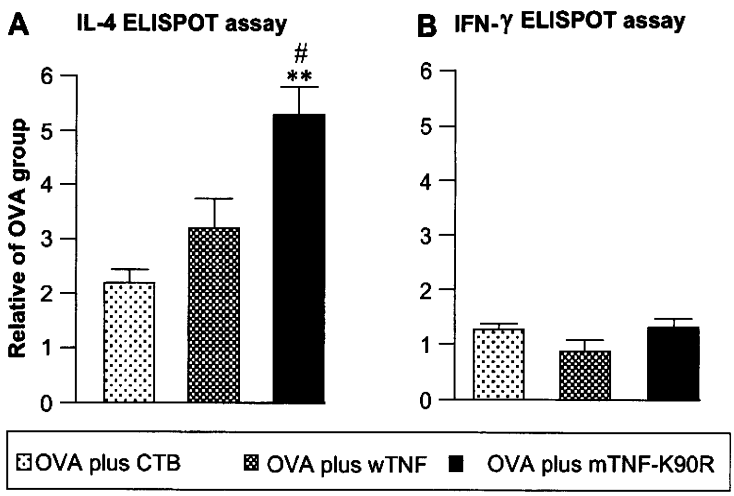

Fig. 4. Analysis of OVA-specific cytokine-secreting cells in mice nasally immunized with OVA plus adjuvant. BALB/c mice were intranasally immunized with OVA alone, OVA plus 1 μg CTB, OVA plus 1 μg wTNF-α or OVA plus 1 μg mTNF-K90R once a week for three consecutive weeks. One week after the last immunization, splenocytes from each group were cultured with 1 mg ml^{-1} OVA. The levels of OVA-specific IL-4 (a) and IFN-γ-producing cells (b) were examined by individual cytokine-specific ELISPOT assay. Data are presented as means ± SEM ($n = 3$; $^{**}P < 0.01$ *versus* value for OVA plus CTB treated group by ANOVA; $^{\#}P < 0.05$ *versus* value for OVA plus wTNF-α treated group by ANOVA).